arXiv:1407.5604v1 [math.NA] 21 Jul 2014

WEAK GALERKIN METHOD FOR THE COUPLED DARCY-STOKES FLOW

WENBIN CHEN, FANG WANG, AND YANQIU WANG

Abstract. A family of weak Galerkin finite element discretization is developed for solving the coupled Darcy-Stokes equation. The equation in consideration admits the Beaver-Joseph-Saffman condition on the interface. By using the weak Galerkin approach, in the discrete space we are able to impose the normal continuity of velocity explicitly. Or in other words, strong coupling is achieved in the discrete space. Different choices of weak Galerkin finite element spaces are discussed, and error estimates are given.

1. Introduction

The goal of this paper is to propose and analyze a weak Galerkin finite element discretization for the coupled Darcy-Stokes equation. The coupled Darcy-Stokes problem has many applications. Readers may refer to the nice overview [12] and references therein for its physical background, modeling, and common numerical methods. To solve the coupled Darcy-Stokes equation numerically, one must address two important issues: how to approximate the Darcy-Stokes interface conditions and how to couple the discretization on both the Darcy side and the Stokes side. Below we shall briefly state how these two issues will be addressed in the proposed weak Galerkin method.

In this paper, we consider the Beavers-Joseph-Saffman (BJS) interface condition [38, 21, 22, 23, 34], which is easier to handle than the original Beavers-Joseph interface condition [2], as the BJS condition will generate a coercive bilinear form in the variational formulation. The BJS interface condition works well when the flow in the porous region is small comparing to the Stokes flow, around the interface.

In the Darcy region, one can use either the primal formulation, which only involves the pressure, or the mixed formulation, which involves both the flux and the pressure, to model the problem. Here we choose the mixed formulation, which has been studied in [1, 3, 11, 15, 16, 17, 24, 25, 26, 29, 36, 37]. In [26], rigorous analysis of the mixed formulation and its weak existence have been presented. According to whether the normal continuity of the velocity is explicitly enforced on the interface or not, two different formulations are proposed in [26]: a strongly coupled formulation and a weakly coupled formulation. Various numerical discretizations have been developed for these two mixed formulations: the work in [16, 17, 26] are based on the weakly coupled formulation, while the work in [1, 11, 25, 24, 36, 37] are based on the strongly coupled formulation. We will adopt the strongly coupled formulation in this paper, which imposes the normal continuity of the velocity strongly in the functional space. Finally, it is also worth mentioning that a different treatment of

1991 *Mathematics Subject Classification.* 65N15, 65N30, 76D07.
Key words and phrases. coupled Darcy-Stokes equation, weak Galerkin method.

the interface condition in the variational formulation is to use the idea of mortar elements, which gives a "strong" but not pointwise coupling [3, 15, 29].

For the discretization of both the Darcy side and the Stokes side, we use the weak Galerkin finite element. The weak Galerkin method was recently introduced in [39] for second order elliptic equations. It is an extension of the standard Galerkin finite element method where classical derivatives were substituted by weakly defined derivatives on functions with discontinuity. Optimal order of a priori error estimates has been observed and established for various weak Galerkin discretization schemes for second order elliptic equations [39, 40, 31]. Numerical implementations of weak Galerkin were discussed in [33, 31] for some model problems. Although the method is still very new, it has already demonstrated many nice properties in various cases [39, 30, 40, 31]. One important advantage of the weak Galerkin method is that, with stabilization, it can be constructed on polytopal meshes, i.e., meshes consisting of arbitrary polygons/polyhedra satisfying certain shape-regularity conditions.

The weak Galerkin method for the mixed formulation of Darcy flow and the weak Galerkin method for the Stokes flow have been individually studied in [40] and [41]. It seems that one only needs to combine these two discretizations together, in order to derive a discretization for the coupled problem. However, it turns out that the discretization for the coupled Darcy-Stokes equations is not that simple. First, due to the interface condition, the formulation of the Stokes side for the coupled Darcy-Stokes equation involves the symmetric full stress tensor, and hence is different from the formulation used in [41]. Consequently, one needs to use the Korn's inequality and the discrete Korn's inequality in the analysis, which is one of the difficulties to be solved in this paper. Because of this, some discrete spaces we will use for the Stokes side are also different from the family proposed in [41]. Second, since we need to prove the discrete inf-sup condition on the entire computational domain, the discrete spaces we choose for the Darcy side are completely different from the family proposed in [40]. Finally, we mention that, in order to impose the interface condition strongly, there must be certain constraints on choosing the Darcy and Stokes side discretizations. For the weak Galerkin method, this can be solved by using the same discrete space on edges for both the Darcy and Stokes side.

Another important issue in discretizing the coupled Darcy-Stokes equation is whether one can use a unified discretization for both the Darcy and Stokes sides, which can greatly simplify the numerical simulation. Previous work on unified discretizations include conforming finite element methods [1], non-conforming finite element methods [25], discontinuous Galerkin methods [36, 37], and $H(div)$ conforming discontinuous Galerkin methods [24]. In this paper, we study several different families of weak Galerkin discretizations in one single framework for the coupled Darcy-Stokes equations, in which the choice of different discretization spaces are controlled by a few parameters denoting the degree of polynomials. Some of these choices will yield unified discretization for both the Darcy-Stokes side.

We would also like to mention a few other works on the coupled Darcy-Stokes equations. The coupled system with the more general interface condition, the Beavers-Joseph condition, has been studied in [6, 7, 8]. Domain decomposition solvers have been studied by different research groups in [6, 10, 13]. Also, a two-grid solver has been studied in [35].

For simplicity, we only consider the two dimensional coupled Darcy-Stokes equation. It is not hard to extend the analysis into three dimensions. The paper is

organized as follows. Section 2 is devoted to the introduction of the model problem and some notations. In Section 3, we present the weak Galerkin discretization for the coupled Darcy-Stokes equation and prove the existence and uniqueness of the discrete solution. Also in this section, some technique tools are presented, which will be used in the error analysis. In Section 4, error estimates for the weak Galerkin solution are given. And finally, in Section 5, numerical results are reported.

2. Model problem and notation

We follow the same notation system and model problem set-up as in [11]. For reader's convenience, the details are presented below.

Consider the flow in a domain $\Omega \in \mathbb{R}^2$ consisting of a Stokes sub-region Ω_S and a porous sub-region Ω_D. Denote by $\boldsymbol{u}$ the velocity and p the pressure. On the Stokes side, the symmetric strain and stress tensors are defined, respectively, by $D(\boldsymbol{u}) = \frac{1}{2}(\nabla \boldsymbol{u} + \nabla \boldsymbol{u}^T)$ and $\mathbb{T}(\boldsymbol{u}, p) = 2\nu D(\boldsymbol{u}) - pI$, where the given constant $\nu > 0$ is the fluid viscosity and I is the identity matrix. On the Darcy side, denote by $\mathbb{K}$ the symmetric positive definite permeability tensor. Moreover, we assume that $\mathbb{K}$ is smooth and uniformly bounded above in Ω_D.

Next we state the coupled Darcy-Stokes equation in Ω. The flow in the Stokes region is governed by the time-independent Stokes equation, while the flow in the porous region is governed by the Darcy equation, i.e.,

$$\begin{aligned} -\nabla \cdot \mathbb{T}(\boldsymbol{u}, p) &= \boldsymbol{f} && \text{in } \Omega_S, \\ \mathbb{K}^{-1}\boldsymbol{u} + \nabla p &= \boldsymbol{f} && \text{in } \Omega_D, \\ \nabla \cdot \boldsymbol{u} &= g && \text{in } \Omega, \end{aligned} \tag{2.1}$$

where $\boldsymbol{f}$ and g are given vector-valued and scalar-valued functions, respectively, in Ω. Such a coupled system has been studied by many researchers.

To complete the problem, interface conditions and boundary conditions need to be imposed. Denote by $\Gamma_{SD} = (\partial\Omega_D) \cap (\partial\Omega_S)$ the interface between the Stokes and Darcy regions, and $\Gamma_S = \partial\Omega_S \backslash \Gamma_{SD}$, $\Gamma_D = \partial\Omega_D \backslash \Gamma_{SD}$ the outer boundary, as shown in Figure 1. Following the convention, we denote by $(\mathbf{n}, \mathbf{t})$ the unit outward normal vector and the unit tangential vector that form a right-hand coordinate system on the boundary of a given domain. On the interface Γ_{SD}, a set of unit normal and unit tangential vectors, $(\hat{\mathbf{n}}, \hat{\mathbf{t}})$, is specified such that $\hat{\mathbf{n}}$ points from Ω_S into Ω_D, as illustrated in Figure 1.

Figure 1. Domain of the coupled Darcy-Stokes problem.

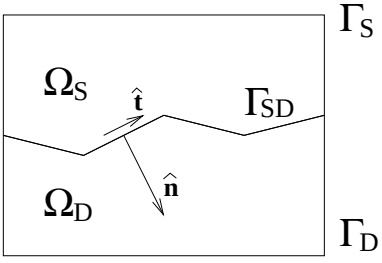

When necessary, we put S and D in the subscript of $\boldsymbol{u}$ and p to distinguish between the Stokes and the Darcy variables, for example, $\boldsymbol{u}_S = \boldsymbol{u}|_{\Omega_S}$ and $p_D =$

$p|_{\Omega_D}$. With the aid of these notations, now we are able to state the boundary and interface conditions. For simplicity, consider the Dirichlet boundary condition on the Stokes side and the Neumann boundary condition on the Darcy side:

$$\begin{aligned} &\boldsymbol{u}_S = \mathbf{0} && \text{on } \Gamma_S, \\ &\boldsymbol{u}_D \cdot \mathbf{n} = 0 && \text{on } \Gamma_D. \end{aligned} \tag{2.2}$$

In order to guarantee the uniqueness of the velocity, we assume that $\Gamma_S \neq \emptyset$. When using the mixed finite element method to discretize system (2.1), both boundary conditions in (2.2) are essential, and thus are easier to handle in the rest of the paper. We point out that our analysis can be easily extended to natural boundary conditions, i.e., Neumann boundary condition on the Stokes side and Dirichlet boundary condition on the Darcy side, as well as other possible type of boundary conditions.

The interface conditions are defined on Γ_{SD} and consist of three parts [2, 38]:

$$\boldsymbol{u}_S \cdot \hat{\mathbf{n}} = \boldsymbol{u}_D \cdot \hat{\mathbf{n}}, \tag{2.3}$$

$$-\mathbb{T}(\boldsymbol{u}_S, p_S)\hat{\mathbf{n}} \cdot \hat{\mathbf{n}} = p_D, \tag{2.4}$$

$$-\mathbb{T}(\boldsymbol{u}_S, p_S)\hat{\mathbf{n}} \cdot \hat{\mathbf{t}} = \mu \mathbb{K}^{-1/2} \boldsymbol{u}_S \cdot \hat{\mathbf{t}}, \tag{2.5}$$

where (2.5) is the famous Beavers-Joseph-Saffman condition, in which $\mu > 0$ is an experimentally determined coefficient. We assume that μ is smooth and uniformly bounded both above and away from zero. Conditions (2.4) and (2.5) can be combined into one:

$$\mathbb{T}(\boldsymbol{u}_S, p_S)\hat{\mathbf{n}} + p_D\hat{\mathbf{n}} + \mu \mathbb{K}^{-1/2} (\boldsymbol{u}_S \cdot \hat{\mathbf{t}})\hat{\mathbf{t}} = 0 \qquad \text{on } \Gamma_{SD}. \tag{2.6}$$

By the divergence theorem, the homogeneous boundary condition (2.2) requires that g satisfies a compatibility condition $\int_\Omega g\, dx = 0$. It is also obvious that the pressure p is unique only up to a constant. Hence we conveniently assume that

$$\int_\Omega p\, dx = 0.$$

Throughout this paper, we consider the the mixed formulation of problem (2.1), which has been studied in details in [18, 26]. Given a polygon K, denote by $H^s(K)$ the usual Sobolev space equipped with the norm $\|\cdot\|_{s,K}$. For $s = 0$, $H^0(K)$ coincides with the square integrable space $L^2(K)$ and we simply denote the L^2 norm on K by $\|\cdot\|_K$. Denote by $(\cdot,\cdot)_K$ and $<\cdot,\cdot>_K$ the L^2 inner-product and the duality form, respectively, in K. When $K = \Omega$, we suppress the subscript K in the norm and the inner-product, for example, $\|\cdot\|_s = \|\cdot\|_{s,\Omega}$, $\|\cdot\| = \|\cdot\|_\Omega$, and $(\cdot,\cdot) = (\cdot,\cdot)_\Omega$. Finally, all the above-defined notations can be easily extended to vector and tensor spaces, using the usual tensor products.

Define the $H(\mathrm{div}, K)$ space and its norm, respectively, by

$$H(\mathrm{div}, K) = \{\boldsymbol{v} \in (L^2(K))^2, \nabla \cdot \boldsymbol{v} \in L^2(K)\},$$

and

$$\|\boldsymbol{v}\|_{H(\mathrm{div}, K)} = (\|\boldsymbol{v}\|_K^2 + \|\nabla \cdot \boldsymbol{v}\|_K^2)^{1/2}.$$

The trace of functions in $H(\mathrm{div}, K)$ is a subtle issue and has been discussed in many classical works [19, 28]. Let $\Gamma \subset \partial K$. We start from defining

$$H^1_{0,\Gamma}(K) = \{v \in H^1(K), v = 0 \text{ on } \Gamma\}.$$

For all $v \in H^1_{0,\Gamma}(K)$, it is well-known by the trace theorem that $v|_{\partial K\backslash\Gamma} \in H^{1/2}_{00}(\partial K\backslash\Gamma)$, where $H^{1/2}_{00}(\partial K\backslash\Gamma)$ is a subspace of $H^{1/2}(\partial K\backslash\Gamma)$ consisting of functions that can be extended by 0 to $H^{1/2}(\partial K)$. Readers can refer to [19, 28] for more details. For any function $\boldsymbol{v} \in H(\text{div}, K)$, by the trace theorem one has $\boldsymbol{v}\cdot\mathbf{n}|_{\partial K} \in H^{-1/2}(\partial K)$. However, $\boldsymbol{v}\cdot\mathbf{n}$ may not be well-defined on a subset of ∂K. One needs to use the dual space of $H^{1/2}_{00}$ in order to obtain a rigorous definition of the trace. Define

$$H_{0,\Gamma}(\text{div}, K) = \{\boldsymbol{v} \in H(\text{div}, K), \boldsymbol{v}\cdot\mathbf{n} = 0 \text{ on } \Gamma\},$$

where $\boldsymbol{v}\cdot\mathbf{n} = 0$ is in the sense of $\boldsymbol{v}\cdot\mathbf{n} \in (H^{1/2}_{00}(\Gamma))^*$. When $\Gamma = \partial K$, we simply denote $H_{0,\partial K}(\text{div}, K) = H_0(\text{div}, K)$ and $H^1_{0,\partial K}(K) = H^1_0(K)$.

Now we are able to introduce the mixed variational formulation for system (2.1)-(2.5). To this end, we start from defining the spaces for the velocity and the pressure, respectively, by

$$\boldsymbol{V} = \{\boldsymbol{v} \in H_0(\text{div}, \Omega) \,|\, \boldsymbol{v}_S \in H^1(\Omega_S)^2 \text{ and } \boldsymbol{v}|_{\Gamma_S} = \mathbf{0}\},$$
$$\Psi = L^2_0(\Omega) \triangleq \{q \in L^2(\Omega) \,|\, \int_\Omega q\, dx = 0\}.$$

It is not hard to see that $\boldsymbol{V}$ and Ψ, equipped with the norms $(\|\boldsymbol{v}\|^2_{1,\Omega_S} + \|\boldsymbol{v}\|^2_{H(\text{div},\Omega_D)})^{1/2}$ and $\|q\|$ respectively, are both Hilbert spaces. An important property of $\boldsymbol{V}$ is that, all functions in $\boldsymbol{V}$ explicitly satisfy the interface condition (2.3), according to the properties [5] of $H(\text{div}, \Omega)$.

Define bilinear forms $a(\cdot,\cdot) : \boldsymbol{V}\times\boldsymbol{V} \to \mathbb{R}$ and $b(\cdot,\cdot) : \boldsymbol{V}\times\Psi \to \mathbb{R}$ by

$$a(\boldsymbol{u},\boldsymbol{v}) = a_S(\boldsymbol{u},\boldsymbol{v}) + a_D(\boldsymbol{u},\boldsymbol{v}) + a_I(\boldsymbol{u},\boldsymbol{v}),$$
$$b(\boldsymbol{v}, q) = -(\nabla\cdot\boldsymbol{v}, q),$$

where

$$a_S(\boldsymbol{u},\boldsymbol{v}) = 2\nu(D(\boldsymbol{u}), D(\boldsymbol{v}))_{\Omega_S},$$
$$a_D(\boldsymbol{u},\boldsymbol{v}) = (\mathbb{K}^{-1}\boldsymbol{u},\boldsymbol{v})_{\Omega_D},$$
$$a_I(\boldsymbol{u},\boldsymbol{v}) = <\mu\mathbb{K}^{-1/2}\boldsymbol{u}_s\cdot\hat{\mathbf{t}}, \boldsymbol{v}_s\cdot\hat{\mathbf{t}}>_{\Gamma_{SD}}.$$

The mixed variational formulation of the coupled Darcy-Stokes equation can be written as: *Find* $(\boldsymbol{u}, p) \in \boldsymbol{V}\times\Psi$ *such that*

$$\begin{cases} a(\boldsymbol{u},\boldsymbol{v}) + b(\boldsymbol{v}, p) = (\boldsymbol{f},\boldsymbol{v}) & \text{for all } \boldsymbol{v}\in\boldsymbol{V}, \\ b(\boldsymbol{u}, q) = -(g, q) & \text{for all } q\in\Psi. \end{cases} \tag{2.7}$$

In [26], Layton, Schieweck and Yotov has proved the equivalence between (2.7) and (2.1)-(2.5), as well as the existence and uniqueness of the solution to (2.7).

3. Weak Galerkin discretization

In this section, we discuss the weak Galerkin discretization for the coupled Darcy-Stokes problem (2.1)-(2.5). For simplicity of notation, throughout the paper, we use "$\lesssim$" to denote "less than or equal to up to a general constant independent of the mesh size or functions appearing in the inequality". But "$\lesssim$" may depend on ν, $\mathbb{K}$, μ, Ω or Γ_{SD}.

Let $\mathcal{T}_h$ be a polygonal mesh defined on Ω satisfying the shape regularity conditions proposed in [32, 40], in order to guarantee the existence of the usual trace inequality, inverse inequality, and the approximability of polynomials on polygons. We require that $\mathcal{T}_h$ be aligned with Γ_{SD}. For each polygon $K \in \mathcal{T}_h$, denote by K_0

and ∂K the interior and the boundary of K, respectively. Also, denote by h_K the diameter of the element K, and set $h = \max_{K\in\mathcal{T}_h} h_K$. Denote by $\mathcal{T}_h^S$ and $\mathcal{T}_h^D$ the restriction of $\mathcal{T}_h$ in Ω_S and Ω_D, respectively.

Denote by $\mathcal{E}_h$ the set of all edges in $\mathcal{T}_h$. For each edge $e \in \mathcal{E}_h$, denote by h_e its length. Let $\mathcal{E}_h^{SD}$ be the set of all edges in $\mathcal{T}_h \cap \Gamma_{SD}$, and let $\mathcal{E}_h^S$, $\mathcal{E}_h^D$ be the set of all edges in $\mathcal{T}_h \cap (\Omega_S \cup \Gamma_S)$, $\mathcal{T}_h \cap (\Omega_D \cup \Gamma_D)$, respectively. We also denote $\mathcal{E}_{0,h}^S$ and $\mathcal{E}_{0,h}^D$ to be the set of edges interior to Ω_S and Ω_D, respectively.

Let j be a non-negative integer. On each $K \in \mathcal{T}_h$, denote by $P_j(K_0)$ or $P_j(K)$ the set of polynomials with degree less than or equal to j. Likewise, on each $e \in \mathcal{E}_h$, $P_j(e)$ is the set of polynomials of degree no more than j. Following [40, 41], we define the weak Galerkin spaces:

$$\begin{aligned}\boldsymbol{V}_h = \{\boldsymbol{v} = \{\boldsymbol{v}_0, \boldsymbol{v}_b\} : \quad & \boldsymbol{v}_0|_{K_0} \in [P_{\alpha_S}(K_0)]^2 \text{ for } K \in \mathcal{T}_h^S,\\ & \boldsymbol{v}_b|_e \in [P_\beta(e)]^2 \text{ for } e \in \mathcal{E}_h^S \cup \mathcal{E}_h^{SD},\\ & \boldsymbol{v}_0|_{K_0} \in [P_{\alpha_D}(K_0)]^2 \text{ for } K \in \mathcal{T}_h^D,\\ & \boldsymbol{v}_b|_e = v_b \mathbf{n}_e \text{ where } v_b \in P_\beta(e) \text{ for } e \in \mathcal{E}_h^D,\\ & \boldsymbol{v}_b|_e = 0 \text{ for } e \in \mathcal{E}_h \cap \partial\Omega\},\end{aligned}$$

where α_S, α_D and β are non-negative integers, $\mathbf{n}_e$ is a prescribed normal direction for edge $e \in \mathcal{E}_h^D$, and

$$\Psi_h = \{q \in L_0^2(\Omega) : q|_K \in P_{\gamma_S}(K) \text{ for } K \in \mathcal{T}_h^S \text{ and } q|_K \in P_{\gamma_D}(K) \text{ for } K \in \mathcal{T}_h^D\},$$

where γ_S and γ_D are non-negative integers. Moreover, assume that

$$\begin{aligned}&\beta - 1 \le \gamma_S \le \beta \le \alpha_S \le \beta + 1,\\ &\beta - 1 \le \gamma_D \le \beta = \alpha_D,\\ &\alpha_S \le \gamma_S + 1.\end{aligned} \tag{3.1}$$

Later we shall discuss more about the choice of parameters α_S, α_D, β, γ_S, and γ_D. But let use first give two examples that satisfy (3.1), both providing unified discretizations for both the Darcy and Stokes sides:

Example 1: Set $\alpha_S = \alpha_D = \beta = \gamma_S = \gamma_D = j$ where $j \ge 1$;
Example 2: Set $\alpha_S = \alpha_D = \beta = j$ and $\gamma_S = \gamma_D = j - 1$, where $j \ge 1$.

Remark 3.1. *Condition (3.1) is derived from certain constraints on constructing weak Galerkin spaces, which will become clear after defining the weak gradient, the weak divergence and the well-posedness of the discrete system. Indeed, a minimum set of conditions on the parameters looks like*

$$\begin{aligned}&\beta - 1 \le \gamma_S \le \beta \le \alpha_S \le \beta + 1,\\ &\beta - 1 \le \gamma_D \le \beta \le \alpha_D \le \beta + 1,\\ &\alpha_S \le \gamma_S + 1, \qquad \alpha_D \le \gamma_D + 1,\end{aligned} \tag{3.2}$$

which is more general than Condition (3.1). However, when performing the error analysis we realized that, by enforcing $\alpha_D = \beta$, the theoretical error estimate in terms of γ_D is one order higher than in the case of $\alpha_D > \beta$. Hence in this paper we shall focus on the case $\alpha_D = \beta$. Note that Condition (3.2) combined with $\alpha_D = \beta$ gives exactly Condition (3.1).

Note that for both the Stokes side and the Darcy side, we deliberately set $\boldsymbol{v}_b$ to have the same polynomial degree, which ensures seamless transition on the Darcy-Stokes interface. The spaces defined above are different from the spaces introduced in [40, 41], which are designed for the Darcy flow and for the Stokes equations individually. This is because we have found, while working on the theoretical analysis, that the spaces in [40, 41] may not be suitable for discretizing the coupled Darcy-Stokes equation. Therefore, we have to construct a new set of spaces $\boldsymbol{V}_h$ and Ψ_h.

Next, we define the weak gradient and the weak divergence on $\boldsymbol{V}_h$. Both of them are defined element-wisely. For each $K \in \mathcal{T}_h$ and $\boldsymbol{v} = \{\boldsymbol{v}_0, \boldsymbol{v}_b\}$, define the weak gradient $\nabla_w \boldsymbol{v}|_K \in [P_\beta(K)]^{2\times 2}$ and weak divergence $\nabla_w \cdot \boldsymbol{v} \in P_\beta(K)$, respectively, by

$$(\nabla_w \boldsymbol{v}, \tau)_K = -(\boldsymbol{v}_0, \nabla \cdot \tau)_K + < \boldsymbol{v}_b, \tau \mathbf{n} >_{\partial K} \qquad \text{for all } \tau \in [P_\beta(K)]^{2\times 2}, \tag{3.3}$$

$$(\nabla_w \cdot \boldsymbol{v}, q)_K = -(\boldsymbol{v}_0, \nabla q)_K + < \boldsymbol{v}_b \cdot \mathbf{n}, q >_{\partial K} \qquad \text{for all } q \in P_\beta(K). \tag{3.4}$$

Note that the weak gradient is only needed on $K \in \mathcal{T}_h^S$, while the weak divergence is needed on both $K \in \mathcal{T}_h^S$ and $K \in \mathcal{T}_h^D$. By the definition of the space $\boldsymbol{V}_h$, when an edge e of $K \in \mathcal{T}_h^D$ lies in $\mathcal{E}_h^D$, we have $\boldsymbol{v}_b = v_b \mathbf{n}_e$ where $v_b \in P_\beta(e)$ on this edge; and when an edge e of $K \in \mathcal{T}_h^D$ lies in $\mathcal{E}_h^{SD}$, we have $\boldsymbol{v}_b \in [P_\beta(e)]^2$ on this edge. In both cases, $\boldsymbol{v}_b \cdot \mathbf{n} \in P_\beta(e)$ and thus the definition of the weak divergence in (3.4) is consistent on all $K \in \mathcal{T}_h$.

Denote

$$D_w(\boldsymbol{v}) = \frac{1}{2}\left(\nabla_w \boldsymbol{v} + (\nabla_w \boldsymbol{v})^T\right).$$

On each $K \in \mathcal{T}_h$, denote by Q_0 the L^2 projection onto $(P_{\alpha_S}(K))^2$ or $(P_{\alpha_D}(K))^2$, depending on whether K is in $\mathcal{T}_h^S$ or T_h^D. On each $e \in \mathcal{E}_h$, denote by Q_b the L^2 projection onto $(P_\beta(e))^2$ or $P_\beta(e)\mathbf{n}$, depending on whether e is on the Stokes side or the Darcy side. On the Stokes side including the interface, Q_b operates on both components of the velocity, while on the Darcy side, it only operates on the normal components of the velocity. On the interface Γ_{SD}, the normal component of the velocity is continuous and thus Q_b transits naturally between the Darcy and the Stokes subdomains. Combining these local projections together, we can define an L^2 projection $Q_h = \{Q_0, Q_b\}$ onto $\boldsymbol{V}_h$. Similarly, denote by $\mathbb{Q}_h$ the L^2 projection onto Ψ_h. Now we can define the bilinear forms

$$a_h(\boldsymbol{u}, \boldsymbol{v}) = a_{h,S}(\boldsymbol{u}, \boldsymbol{v}) + a_{h,D}(\boldsymbol{u}, \boldsymbol{v}) + a_I(\boldsymbol{u}, \boldsymbol{v}) \qquad \text{for } \boldsymbol{u}, \boldsymbol{v} \in \boldsymbol{V}_h,$$

$$b_h(\boldsymbol{v}, q) = -(\nabla_w \cdot \boldsymbol{v}, q) \qquad \text{for } \boldsymbol{v} \in \boldsymbol{V}_h \text{ and } q \in \Psi_h,$$

where

$$a_S(\boldsymbol{u}, \boldsymbol{v}) = 2\nu(D_w(\boldsymbol{u}), D_w(\boldsymbol{v}))_{\Omega_S} + \rho_S \sum_{K \in \mathcal{T}_h^S} h_K^{-1} < Q_b \boldsymbol{u}_0 - \boldsymbol{u}_b, Q_b \boldsymbol{v}_0 - \boldsymbol{v}_b >_{\partial K},$$

$$a_D(\boldsymbol{u}, \boldsymbol{v}) = (\mathbb{K}^{-1} \boldsymbol{u}_0, \boldsymbol{v}_0)_{\Omega_D} + \rho_D \sum_{K \in \mathcal{T}_h^D} h_K^{-1} < (\boldsymbol{u}_0 - \boldsymbol{u}_b) \cdot \mathbf{n}, (\boldsymbol{v}_0 - \boldsymbol{v}_b) \cdot \mathbf{n} >_{\partial K},$$

$$a_I(\boldsymbol{u}, \boldsymbol{v}) = < \mu \mathbb{K}^{-1/2} \boldsymbol{u}_b \cdot \hat{\mathbf{t}}, \boldsymbol{v}_b \cdot \hat{\mathbf{t}} >_{\Gamma_{SD}},$$

in which ρ_S and ρ_D are positive constants. One can view ρ_S and ρ_D as stabilization parameters, but the good news is that the weak Galerkin method does not depend on these parameters as the discontinuous Galerkin method does. One can simply set $\rho_S = \rho_D = 1$.

The weak Galerkin formulation for the Darcy-Stokes flow can now be written as: find $\boldsymbol{u} \in \boldsymbol{V}_h$ and $p \in \Psi_h$ such that

$$\begin{cases} a_h(\boldsymbol{u}, \boldsymbol{v}) + b_h(\boldsymbol{v}, p) = (\boldsymbol{f}, \boldsymbol{v}_0) & \text{for all } \boldsymbol{v} \in \boldsymbol{V}_h, \\ b_h(\boldsymbol{u}, q) = -(g, q) & \text{for all } q \in \Psi_h. \end{cases} \tag{3.5}$$

We shall analyze the well-posedness and approximation properties of the weak Galerkin discretization (3.5).

Remark 3.2. *The bilinear form $a_h(\boldsymbol{u}, \boldsymbol{v})$ contains a stabilization part, and for convenience, we denote it by*

$$\begin{aligned} s(\boldsymbol{u}, \boldsymbol{v}) = \rho_S \sum_{K \in \mathcal{T}_h^S} h_K^{-1} < Q_b \boldsymbol{u}_0 - \boldsymbol{u}_b, Q_b \boldsymbol{v}_0 - \boldsymbol{v}_b >_{\partial K} \\ + \rho_D \sum_{K \in \mathcal{T}_h^D} h_K^{-1} < (\boldsymbol{u}_0 - \boldsymbol{u}_b) \cdot \mathbf{n}, (\boldsymbol{v}_0 - \boldsymbol{v}_b) \cdot \mathbf{n} >_{\partial K} . \end{aligned}$$

3.1. **Discrete norm.** Define a discrete norm on $\boldsymbol{V}_h$ by

$$\begin{aligned} \|\boldsymbol{v}\|_{\boldsymbol{V}_h} = \Big(& 2\nu \|D_w(\boldsymbol{v})\|_{\Omega_S}^2 + \rho_S \sum_{K \in \mathcal{T}_h^S} h_K^{-1} \|Q_b \boldsymbol{v}_0 - \boldsymbol{v}_b\|_{\partial K}^2 \\ & + \|\mathbb{K}^{-1/2} \boldsymbol{v}_0\|_{\Omega_D}^2 + \rho_D \sum_{K \in \mathcal{T}_h^D} h_K^{-1} \|(\boldsymbol{v}_0 - \boldsymbol{v}_b) \cdot \mathbf{n}\|_{\partial K}^2 \\ & + \|\nabla_w \cdot \boldsymbol{v}\|_{\Omega}^2 + \|\mu^{1/2} \mathbb{K}^{-1/4} \boldsymbol{v}_b \cdot \hat{\mathbf{t}}\|_{\Gamma_{SD}}^2 \Big)^{1/2}. \end{aligned}$$

It is obvious that $a_h(\boldsymbol{v}, \boldsymbol{v}) = \|\boldsymbol{v}\|_{\boldsymbol{V}_h}^2$. The discrete norm on Ψ_h inherits the norm on Ψ, which is just the L^2 norm. Denote $|||\cdot||| = \|\cdot\|_{\boldsymbol{V}_h \times \Psi_h}$. We shall prove that $\|\cdot\|_{\boldsymbol{V}_h}$ is a well-defined norm for certain choices of parameters α_S, α_D, β, γ_S and γ_D. To this end, we only need to show that $\|\boldsymbol{v}\|_{\boldsymbol{V}_h} = 0$ implies $\boldsymbol{v} \equiv 0$ for $\boldsymbol{v} \in \boldsymbol{V}_h$. By definition, $\|\boldsymbol{v}\|_{\boldsymbol{V}_h} = 0$ indicates that

$$D_w(\boldsymbol{v}) = \mathbf{0} \text{ on } K \in \mathcal{T}_h^S, \qquad Q_b \boldsymbol{v}_0 - \boldsymbol{v}_b = \mathbf{0} \text{ on } e \in \mathcal{E}_h^S \cup \mathcal{E}_h^{SD}, \tag{3.6}$$

$$\boldsymbol{v}_0 = \mathbf{0} \text{ on } K \in \mathcal{T}_h^D, \qquad (\boldsymbol{v}_0 - \boldsymbol{v}_b) \cdot \mathbf{n} = 0 \text{ on } e \in \mathcal{E}_h^D \cup \mathcal{E}_h^{SD}, \tag{3.7}$$

$$\boldsymbol{v}_b \cdot \hat{\mathbf{t}} = 0 \text{ on } e \in \mathcal{E}_h^{SD}. \tag{3.8}$$

By examining these equations and depending on whether $\alpha_S = \beta$ or $\alpha_S = \beta + 1$, we have the following results.

Lemma 3.1. *If $\alpha_S = \beta$, then $\|\cdot\|_{\boldsymbol{V}_h}$ is a well-defined norm on $\boldsymbol{V}_h$.*

Proof From (3.7), it is not hard to see that $\boldsymbol{v}_0$ and $\boldsymbol{v}_b$ vanishes on all $K \in \mathcal{T}_h^D$ and $e \in \mathcal{E}_h^D$. Combining (3.7) and (3.8), we also know that $\boldsymbol{v}_b$ vanishes on Γ_{SD}.

On $K \in \mathcal{T}_h^S$, using the definition (3.3) gives

$$((\nabla_w \boldsymbol{v})^T, \tau)_K = (\nabla_w \boldsymbol{v}, \tau^T)_K = -(\boldsymbol{v}_0, \nabla \cdot \tau^T)_K + < \boldsymbol{v}_b, \tau^T \mathbf{n} >_{\partial K} \quad \text{for all } \tau \in [P_\beta(K)]^{2\times 2},$$

which, combined with (3.3), implies that

$$2(D_w(\boldsymbol{v}), \tau)_K = -(\boldsymbol{v}_0, \nabla \cdot (\tau + \tau^T))_K + < \boldsymbol{v}_b, (\tau + \tau^T)\mathbf{n} >_{\partial K} \quad \text{for all } \tau \in [P_\beta(K)]^{2\times 2}.$$

Therefore, $D_w(\boldsymbol{v}) = \mathbf{0}$ on $K \in \mathcal{T}_h^S$ implies that for all symmetric $\tau \in [P_\beta(K)]^{2\times 2}$,

$$\begin{aligned} 0 &= -(\boldsymbol{v}_0, \nabla\cdot\tau)_K + < \boldsymbol{v}_b, \tau\mathbf{n} >_{\partial K} \\ &= (\nabla \boldsymbol{v}_0, \tau)_K - < \boldsymbol{v}_0 - \boldsymbol{v}_b, \tau\mathbf{n} >_{\partial K} \\ &= (D(\boldsymbol{v}_0), \tau)_K - < Q_b\boldsymbol{v}_0 - \boldsymbol{v}_b, \tau\mathbf{n} >_{\partial K} \\ &= (D(\boldsymbol{v}_0), \tau)_K, \end{aligned}$$

where the last step follows from (3.6). Hence we have $D(\boldsymbol{v}_0) \equiv \mathbf{0}$ on all $K \in \mathcal{T}_h^S$. By the definition of $D(\cdot)$, this in turn implies that $\boldsymbol{v}_0|_K \in RM$ where $RM = span\{\begin{bmatrix}1\\0\end{bmatrix}, \begin{bmatrix}0\\1\end{bmatrix}, \begin{bmatrix}-y\\x\end{bmatrix}\}$ denotes the space of rigid body motions. If we can further show that $\boldsymbol{v}_0$ is continuous on the entire Ω_S, then by the definition of RM it is not hard to see that $\boldsymbol{v}_0|_{\Omega_S} \in RM$.

Now, since $\alpha_S = \beta$, by (3.6) we known that $\boldsymbol{v}_0$ must be continuous in the entire Ω_S. Therefore $\boldsymbol{v}_0|_{\Omega_S} \in RM$. Note that $\boldsymbol{v}_b$ vanishes on $\partial\Omega_S$, again by (3.6), $\boldsymbol{v}_0$ must also vanish on $\partial\Omega_S$, which implies that $\boldsymbol{v}_0 \equiv \mathbf{0}$ in Ω_S. Consequently, $\boldsymbol{v}_b \equiv \mathbf{0}$ on $e \in \mathcal{E}_h^S \cup \mathcal{E}_h^{SD}$. This completes the proof of the lemma. □

For $\alpha_S = \beta + 1$, the situation is more complicated. Using the same argument as in the proof of Lemma 3.1, for $\alpha_S = \beta + 1$ we can still prove that $\boldsymbol{v}_0 = \boldsymbol{v}_b \equiv \mathbf{0}$ in Ω_D and $\boldsymbol{v}_0|_K \in RM$ for $K \in \mathcal{T}_h^S$. Now, Q_b on the Stokes side is no longer an identity operator, and hence Equation (3.6) only implies that $Q_b\boldsymbol{v}_0$ is continuous across the edges in Ω_S, while $\boldsymbol{v}_0$ is not necessarily continuous. We need to consider two cases separately, the case $\beta \geq 1$ and the case $\beta = 0$.

For $\beta \geq 1$ and $\boldsymbol{v}_0|_K \in RM \subset [P_1(K)]^2$, we can still get $Q_b\boldsymbol{v}_0 = \boldsymbol{v}_0$ on edges, which together with the continuity of $Q_b\boldsymbol{v}_0$ across edges implies that $\boldsymbol{v}_0$ is continuous in the entire Ω_S. Thus $\boldsymbol{v}_0|_{\Omega_S} \in RM$. The rest is similar to the proof of Lemma 3.1 and is summarized in the following lemma:

Lemma 3.2. *If $\alpha_S = \beta + 1$ and $\beta \geq 1$, then $\|\cdot\|_{\boldsymbol{V}_h}$ is a well-defined norm on $\boldsymbol{V}_h$.*

Finally, we consider the case of $\alpha_S = \beta + 1$ and $\beta = 0$. When $\beta = 0$, Equation (3.6) implies that $\boldsymbol{v}_0$ is continuous only at the center of internal edges in $\mathcal{T}_h^S$. On boundary edges $e \in \mathcal{E}_h \cap \partial\Omega_S$, the value of $\boldsymbol{v}_0$ at the center is equal to the value of $\boldsymbol{v}_b$, which is $\mathbf{0}$. If $\mathcal{T}_h^S$ is a triangular mesh, clearly $\boldsymbol{v}_0$ can be viewed as in the space of the lowest order Crouzeix-Raviart non-conforming finite element defined on the triangular mesh $\mathcal{T}_h^S$ with zero boundary condition. In this case, Falk [14] has shown, using dimension counting, that $\boldsymbol{v}_0 \in RM$ on all $K \in \mathcal{T}_h^S$ is not enough to guarantee $\boldsymbol{v}_0 \equiv \mathbf{0}$. This is just the famous result that the lowest order Crouzeix-Raviart non-conforming finite element does not satisfy the discrete Korn's inequality.

However, the situation can be different when the mesh contains general polygons. To analyze this, we first introduce a few tools.

Lemma 3.3. *Let $\boldsymbol{v}_0 \in RM$ on a polygon K. If $\boldsymbol{v}_0$ vanishes on two different points in K, then $\boldsymbol{v}_0 \equiv \mathbf{0}$.*

Proof Any $\boldsymbol{v}_0 \in RM$ can be written as $\begin{bmatrix}a - cy\\ b + cx\end{bmatrix}$. Two different points either have different x-coordinates or y-coordinates. If $\boldsymbol{v}_0$ vanishes on both points, it is not hard to see that c must be 0. Consequently, a and b must also be 0. This completes the proof of the lemma. □

Algorithm 3.1. *We start from setting all polygons in $\mathcal{T}_h^S$ black.*

(1) *For all $K \in \mathcal{T}_h^S$, set K white if K has two different edges lying on $\partial\Omega_S$;*
(2) *For all black polygons,*
   - *Set polygon K white if K has one edge lying on $\partial\Omega_S$ and shares another edge with a white polygon;*
   - *Set polygon K white if K shares two edges with other white polygons;*
(3) *Repeat Step 2 until there is no new coloring.*

Definition 3.1. *Mesh $\mathcal{T}_h^S$ is colorable if Algorithm 3.1 will turn all polygons in $\mathcal{T}_h^S$ white. Otherwise, it is not colorable.*

Clearly, a simple example of colorable mesh is the rectangular grid. We know that $\boldsymbol{v}_0$ vanishes at the center of each $e \in \mathcal{E}_h \cap \partial\Omega_S$. Thus, the property stated in Lemma 3.3 can propagate to all white polygons generated by Algorithm 3.1. This leads to the following conclusion:

Theorem 3.1. *When $\beta = 0$ and $\alpha_S = 1$, if $\mathcal{T}_h^S$ is colorable, then $\|\cdot\|_{\boldsymbol{V}_h}$ is a well-defined norm.*

Remark 3.3. *In the rest of this paper, when $\beta = 0$ and $\alpha_S = 1$, we always assume that the mesh is colorable. In other words, $\|\cdot\|_{\boldsymbol{V}_h}$ is always well-defined in this paper.*

3.2. **Existence and uniqueness of the discrete solution.** Given that $\|\cdot\|_{\boldsymbol{V}_h}$ is a well-defined norm in $\boldsymbol{V}_h$, we can easily derive the existence and uniqueness of the solution to System (3.5).

Theorem 3.2. *System (3.5) admits a unique solution.*

Proof For discrete problems, uniqueness implies existence of the solution. Therefore we only need to prove that when $\boldsymbol{f} \equiv \boldsymbol{0}$ and $q \equiv 0$, the solution to (3.5) is exactly zero. By setting $\boldsymbol{v} = \boldsymbol{u}$ and $q = p$ and subtracting the two equations in (3.5), one has $0 = a_h(\boldsymbol{u}, \boldsymbol{u}) = \|\boldsymbol{u}\|_{\boldsymbol{V}_h}^2$, which clearly implies $\boldsymbol{u} \equiv \boldsymbol{0}$.

Next, by using $0 = b_h(\boldsymbol{v}, p) = -(\nabla_w \cdot \boldsymbol{v}, p)$ for all $\boldsymbol{v} \in \boldsymbol{V}_h$, we will show that $p \equiv 0$ on the entire Ω. Since $\gamma_S \leq \beta$ and $\gamma_D \leq \beta$, by (3.4) we have for all $\boldsymbol{v} \in \boldsymbol{V}_h$

$$0 = (\nabla_w \cdot \boldsymbol{v}, p) = \sum_{K \in \mathcal{T}_h} \left(-(\boldsymbol{v}_0, \nabla p)_K + < \boldsymbol{v}_b \cdot \mathbf{n}, p >_{\partial K}\right). \tag{3.9}$$

By setting $\boldsymbol{v}_b = \boldsymbol{0}$ on all edges and let $\boldsymbol{v}_0$ vanish on all except for one polygon in $\mathcal{T}_h$, one gets

$$(\boldsymbol{v}_0, \nabla p)_K = 0 \text{ for all } \boldsymbol{v} \in \boldsymbol{V}_h \text{ and } K \in \mathcal{T}_h.$$

Note that for polygons lying on either the Darcy side or the Stokes side, according to the definition of $\boldsymbol{V}_h$ and Ψ_h, the space of ∇p is always contained in the space of $\boldsymbol{v}_0$. Thus we conclude that $\nabla p|_K = \boldsymbol{0}$ for all $K \in \mathcal{T}_h$, which implies that p is piecewise constant.

Next, let $\boldsymbol{v}_0 \equiv \boldsymbol{0}$ in Equation (3.9), we have for all $\boldsymbol{v}_b$

$$0 = \sum_{K \in \mathcal{T}_h} < \boldsymbol{v}_b \cdot \mathbf{n}, p >_{\partial K} = \sum_{e \in \mathcal{E}_h} < \boldsymbol{v}_b \cdot \mathbf{n}, [p] >_e, \tag{3.10}$$

where $[p]$ denotes the jump of p on edge e. On boundary edges, $[p]$ is just defined to be the one-sided value of p. Note that the summation in (3.10) does not need to be distinguished on the Darcy or the Stokes side, because $\boldsymbol{v}_b \cdot \mathbf{n}$ for both the Darcy

side and the Stokes side belongs to the same discrete space. Combining Equation (3.10) with the fact that p is piecewise constant, we conclude that p must be a constant on the entire Ω. And since $p \in L_0^2(\Omega)$, thus $p \equiv 0$. This completes the proof of the theorem. □

3.3. **A few technique tools.** In this subsection we introduce a few technique tools that will be used in the error analysis of the weak Galerkin approximation. First, for any $K \in \mathcal{T}_h$ and e being an edge of K, the following trace inequality is known [32, 40]

$$\|\phi\|_e^2 \lesssim h_K^{-1}\|\phi\|_K^2 + h_K|\phi|_{1,K}^2, \tag{3.11}$$

for all $\phi \in H^1(K)$. Unlike the usual trace inequalities, the inequality (3.11) is prove on polytopal meshes satisfying certain shape regularity conditions [32, 40]. For such meshes, the inverse inequality and the approximation property of L^2 projections onto polynomial spaces have also been proved [32, 40]. These inequalities have the same form as their counterparts on triangular and rectangular meshes. In the rest of this paper, we will use them directly, without special mentioning.

On each $K \in \mathcal{T}_h$, denote by Π_h and π_h the L^2 projections onto $[P_\beta(K)]^{2\times 2}$ and $P_\beta(K)$, respectively. And on the entire Ω, we use the same notations, Π_h and π_h, to denote the combination of all local projections. Then one has

Lemma 3.4. *The projection operators satisfy*

$$\begin{aligned} \nabla_w(Q_h\mathbf{v}) &= \Pi_h(\nabla\mathbf{v}) && \text{for all } \boldsymbol{v} \in [H^1(\Omega)]^2, \\ \nabla_w \cdot (Q_h\boldsymbol{v}) &= \pi_h(\nabla\cdot\mathbf{v}) && \text{for all } \boldsymbol{v} \in H(div,\Omega). \end{aligned}$$

Proof By (3.1), (3.3), the definitions of Q_h and Π_h, clearly for all $\tau \in [P_\beta(K)]^{2\times 2}$ and $K \in \mathcal{T}_h$,

$$\begin{aligned} (\nabla_w(Q_h\boldsymbol{v}),\tau)_K &= -(Q_0\boldsymbol{v},\nabla\cdot\tau)_K + < Q_b\boldsymbol{v},\tau\mathbf{n} >_{\partial K} \\ &= -(\boldsymbol{v},\nabla\cdot\tau)_K + < \boldsymbol{v},\tau\mathbf{n} >_{\partial K} \\ &= (\nabla\boldsymbol{v},\tau)_K = (\Pi_h(\nabla\boldsymbol{v}),\tau)_K. \end{aligned}$$

Similarly, for all $q \in P_\beta(K)$ and $K \in \mathcal{T}_h$,

$$\begin{aligned} (\nabla_w\cdot(Q_h\boldsymbol{v}),q)_K &= -(Q_0\boldsymbol{v},\nabla q)_K + < (Q_b\boldsymbol{v})\cdot\mathbf{n},q >_{\partial K} \\ &= -(\boldsymbol{v},\nabla q)_K + < \boldsymbol{v}\cdot\mathbf{n},q >_{\partial K} \\ &= (\nabla\cdot\boldsymbol{v},q)_K = (\pi_h\nabla\cdot\boldsymbol{v},q)_K. \end{aligned}$$

This completes the proof of the lemma. □

Next we prove the discrete inf-sup condition:

Lemma 3.5. *For all $q \in \Psi_h$, one has*

$$\sup_{\boldsymbol{v}\in\boldsymbol{V}_h} \frac{(\nabla_w\cdot\boldsymbol{v},q)}{\|\boldsymbol{v}\|_{\boldsymbol{V}_h}} \gtrsim \|q\|.$$

Proof It is well known that for all $q \in \Psi_h \subset L_0^2(\Omega)$, there exists a $\boldsymbol{w} \in [H_0^1(\Omega)]^2$ such that $\nabla\cdot\boldsymbol{w} = q$ and $\|\boldsymbol{w}\|_1 \lesssim \|q\|$. Define $\boldsymbol{v} = Q_h\boldsymbol{w}$, then by Lemma 3.4, and the facts that $\gamma_S \le \beta$, $\gamma_D \le \beta$, we have

$$(\nabla_w\cdot\boldsymbol{v},q) = (\pi_h(\nabla\cdot\boldsymbol{w}),q) = (\nabla\cdot\boldsymbol{w},q) = \|q\|^2.$$

Now, we only need to prove that

$$\|\boldsymbol{v}\|_{\boldsymbol{V}_h} \lesssim \|\boldsymbol{w}\|_1.$$

Note that

$$\begin{aligned}\|\boldsymbol{v}\|_{\boldsymbol{V}_h} = \Big(&2\nu\|D_w(Q_h\boldsymbol{w})\|_{\Omega_S}^2 + \rho_S \sum_{K\in\mathcal{T}_h^S} h_K^{-1}\|Q_b(Q_0\boldsymbol{w}) - Q_b\boldsymbol{w}\|_{\partial K}^2 \\ &+ \|\mathbb{K}^{-1/2}Q_0\boldsymbol{w}\|_{\Omega_D}^2 + \rho_D \sum_{K\in\mathcal{T}_h^D} h_K^{-1}\|(Q_0\boldsymbol{w} - Q_b\boldsymbol{w})\cdot\mathbf{n}\|_{\partial K}^2 \\ &+ \|\nabla_w\cdot(Q_h\boldsymbol{w})\|_\Omega^2 + \|\mu^{1/2}\mathbb{K}^{-1/4}(Q_b\boldsymbol{w})\cdot\hat{\mathbf{t}}\|_{\Gamma_{SD}}^2\Big)^{1/2}.\end{aligned}$$

We will check the terms in the above equation one-by-one. First, by Lemma 3.4,

$$\begin{aligned}\|D_w(Q_h\boldsymbol{w})\|_{\Omega_S}^2 &= \|\frac{1}{2}(\nabla_w(Q_h\boldsymbol{w}) + \nabla_w(Q_h\boldsymbol{w})^T)\|_{\Omega_S}^2 = \|\frac{1}{2}(\Pi_h\nabla\boldsymbol{w} + (\Pi_h\nabla\boldsymbol{w})^T)\|_{\Omega_S}^2 \\ &= \|\Pi_h D(\boldsymbol{w})\|_{\Omega_S}^2 \lesssim \|\boldsymbol{w}\|_{1,\Omega_S}^2,\end{aligned}$$

and obviously $\|\mathbb{K}^{-1/2}Q_0\boldsymbol{w}\|_{\Omega_D} \lesssim \|\boldsymbol{w}\|_{\Omega_D}$. Next, by using the properties of Q_h and the inequality (3.11), we have for $K \in \mathcal{T}_h^S$,

$$\begin{aligned}h_K^{-1}\|Q_b(Q_0\boldsymbol{w}) - Q_b\boldsymbol{w}\|_{\partial K}^2 &= h_K^{-1}\|Q_b(Q_0\boldsymbol{w} - \boldsymbol{w})\|_{\partial K}^2 \\ &\le h_K^{-1}\|Q_0\boldsymbol{w} - \boldsymbol{w}\|_{\partial K}^2 \\ &\lesssim h_K^{-2}\|Q_0\boldsymbol{w} - \boldsymbol{w}\|_K^2 + \|\nabla(Q_0\boldsymbol{w} - \boldsymbol{w})\|_K^2 \\ &\lesssim \|\nabla\boldsymbol{w}\|_K^2.\end{aligned}$$

Similarly, one can show that for $K \in \mathcal{T}_h^D$,

$$\begin{aligned}h_K^{-1}\|(Q_0\boldsymbol{w} - Q_b\boldsymbol{w})\cdot\mathbf{n}\|_{\partial K}^2 &\lesssim h_K^{-1}\|Q_0\boldsymbol{w} - Q_b\boldsymbol{w}\|_{\partial K}^2 \\ &\lesssim h_K^{-1}\|Q_0\boldsymbol{w} - \boldsymbol{w}\|_{\partial K}^2 \lesssim \|\nabla\boldsymbol{w}\|_K^2.\end{aligned}$$

By using Lemma 3.4, we have

$$\|\nabla_w\cdot(Q_h\boldsymbol{w})\|_\Omega = \|\pi_h(\nabla\cdot\boldsymbol{w})\|_\Omega \le \|\nabla\cdot\boldsymbol{w}\|_\Omega \le \|\nabla\boldsymbol{w}\|_\Omega.$$

Finally, using the trace inequality,

$$\|\mu^{1/2}\mathbb{K}^{-1/4}(Q_b\boldsymbol{w})\cdot\hat{\mathbf{t}}\|_{\Gamma_{SD}} \lesssim \|Q_b\boldsymbol{w}\|_{\Gamma_{SD}} \le \|\boldsymbol{w}\|_{\Gamma_{SD}} \lesssim \|\boldsymbol{w}\|_{1,\Omega}.$$

Combining all the above, we have $\|\boldsymbol{v}\|_{\boldsymbol{V}_h} \lesssim \|\boldsymbol{w}\|_1$, which completes the proof of the lemma. □

By using Lemma 3.4, we can also prove the following result:

Lemma 3.6. *The solution $\boldsymbol{u}$ and p to problem (2.1) satisfies*

$$a_h(Q_h\boldsymbol{u},\boldsymbol{v}) + b_h(\boldsymbol{v},\mathbb{Q}_h p) = (f,\boldsymbol{v}_0) + s(Q_h\boldsymbol{u},\boldsymbol{v}) + l_S(\boldsymbol{v}) - l_D(\boldsymbol{v}) - l_{div}(\boldsymbol{v}) - l_I(\boldsymbol{v}),$$

for all $\boldsymbol{v} \in \boldsymbol{V}_h$, where the linear functionals $l_S(\cdot)$, $l_D(\cdot)$, $l_{div}(\cdot)$, and $l_I(\cdot)$ are defined by

$$
\begin{aligned}
l_S(\boldsymbol{v}) &= 2\nu \sum_{K\in\mathcal{T}_h^S} < \boldsymbol{v}_0 - \boldsymbol{v}_b, (D(\boldsymbol{u}) - \Pi_h D(\boldsymbol{u}))\mathbf{n} >_{\partial K},\\
l_D(\boldsymbol{v}) &= (\mathbb{K}^{-1}(\boldsymbol{u} - Q_0\boldsymbol{u}), \boldsymbol{v}_0)_{\Omega_D},\\
l_{div}(\boldsymbol{v}) &= \sum_{K\in\mathcal{T}_h} < (\boldsymbol{v}_0 - \boldsymbol{v}_b)\cdot\mathbf{n}, p - \mathbb{Q}_h p >_{\partial K},\\
l_I(\boldsymbol{v}) &=< \mu\mathbb{K}^{-1/2}(\boldsymbol{u}_S - Q_b\boldsymbol{u}_s)\cdot\hat{\mathbf{t}}, \boldsymbol{v}_b\cdot\hat{\mathbf{t}} >_{\Gamma_{SD}}.
\end{aligned}
$$

Proof Testing problem (2.1) with $\boldsymbol{v} = \{\boldsymbol{v}_0, \boldsymbol{v}_b\} \in \boldsymbol{V}_h$ and using integration by parts, one gets

(3.12)

$$
\begin{aligned}
&(\boldsymbol{f}, \boldsymbol{v}_0)\\
&= (-\nabla\cdot(2\nu D(\boldsymbol{u}) - pI), \boldsymbol{v}_0)_{\Omega_S} + (\mathbb{K}^{-1}\boldsymbol{u}, \boldsymbol{v}_0)_{\Omega_D} + (\nabla p, \boldsymbol{v}_0)_{\Omega_D}\\
&= \sum_{K\in\mathcal{T}_h^S}\Big(2\nu(D(\boldsymbol{u}), D(\boldsymbol{v}_0))_K - 2\nu < \boldsymbol{v}_0, D(\boldsymbol{u})\mathbf{n} >_{\partial K}\Big) + (\mathbb{K}^{-1}\boldsymbol{u}, \boldsymbol{v}_0)_{\Omega_D}\\
&\quad + \sum_{K\in\mathcal{T}_h}\Big(- (\nabla\cdot\boldsymbol{v}_0, p)_K + < \boldsymbol{v}_0\cdot\mathbf{n}, p >_{\partial K}\Big)\\
&= \sum_{K\in\mathcal{T}_h^S}\Big(2\nu(D(\boldsymbol{u}), D(\boldsymbol{v}_0))_K - 2\nu < \boldsymbol{v}_0 - \boldsymbol{v}_b, D(\boldsymbol{u})\mathbf{n} >_{\partial K}\Big) + (\mathbb{K}^{-1}\boldsymbol{u}, \boldsymbol{v}_0)_{\Omega_D}\\
&\quad + \sum_{K\in\mathcal{T}_h}\Big(- (\nabla\cdot\boldsymbol{v}_0, p)_K + < (\boldsymbol{v}_0 - \boldsymbol{v}_b)\cdot\mathbf{n}, p >_{\partial K}\Big)\\
&\quad + < \mu\mathbb{K}^{-1/2}\boldsymbol{u}_S\cdot\hat{\mathbf{t}}, \boldsymbol{v}_b\cdot\hat{\mathbf{t}} >_{\Gamma_{SD}},
\end{aligned}
$$

where in the last step we have used $\boldsymbol{v}_b = \mathbf{0}$ on $\partial\Omega$, the interface condition (2.6), and the continuity of $\mathbb{T}(\boldsymbol{u}, p)\mathbf{n}$ and p across the edges in $\mathcal{E}_{0,h}^S$ and $\mathcal{E}_{0,h}^D$, respectively. More specifically, that is

$$
\begin{aligned}
&\sum_{K\in\mathcal{T}_h^S} 2\nu < \boldsymbol{v}_b, D(\boldsymbol{u})\mathbf{n} >_{\partial K} - \sum_{K\in\mathcal{T}_h} < \boldsymbol{v}_b\cdot\mathbf{n}, p >_{\partial K}\\
&= \sum_{K\in\mathcal{T}_h^S} < \boldsymbol{v}_b, \mathbb{T}(\boldsymbol{u}, p)\mathbf{n} >_{\partial K} - \sum_{K\in\mathcal{T}_h^D} < \boldsymbol{v}_b, p\mathbf{n} >_{\partial K}\\
&= \sum_{e\in\mathcal{E}_{0,h}^S} < \boldsymbol{v}_b, [\mathbb{T}(\boldsymbol{u}, p)\mathbf{n}] >_e + \sum_{e\in\mathcal{E}_h^{SD}} < \boldsymbol{v}_b, \mathbb{T}(\boldsymbol{u}, p)\hat{\mathbf{n}} >_e\\
&\quad - \sum_{e\in\mathcal{E}_{0,h}^D} < \boldsymbol{v}_b, [p\mathbf{n}] >_e - \sum_{e\in\mathcal{E}_h^{SD}} < \boldsymbol{v}_b, -p\hat{\mathbf{n}} >_e\\
&= \sum_{e\in\mathcal{E}_h^{SD}} < \boldsymbol{v}_b, \mathbb{T}(\boldsymbol{u}, p)\hat{\mathbf{n}} >_e + \sum_{e\in\mathcal{E}_h^{SD}} < \boldsymbol{v}_b, p\hat{\mathbf{n}} >_e\\
&= - \sum_{e\in\mathcal{E}_h^{SD}} < \boldsymbol{v}_b, \mu\mathbb{K}^{-1/2}(\boldsymbol{u}_S\cdot\hat{\mathbf{t}})\hat{\mathbf{t}} >_e,
\end{aligned}
$$

where $[\cdot]$ denotes the jump, which is a notation borrowed from the discontinuous Galerkin literature.

Now let us compute $a_h(Q_h\boldsymbol{u},\boldsymbol{v})+b_h(\boldsymbol{v},\mathbb{Q}_h p)$, where $\boldsymbol{u}$, p are the solutions to (2.1) and $\boldsymbol{v}\in\boldsymbol{V}_h$. Since $D_w(Q_h\boldsymbol{u})=\Pi_h D(\boldsymbol{u})$ is symmetric and by using the properties of Q_h, we have

$$\begin{aligned}
&a_h(Q_h\boldsymbol{u},\boldsymbol{v})+b_h(\boldsymbol{v},\mathbb{Q}_h p)\\
&=2\nu(D_w(Q_h\boldsymbol{u}),D_w(\boldsymbol{v}))_{\Omega_S}+(\mathbb{K}^{-1}Q_0\boldsymbol{u},\boldsymbol{v}_0)_{\Omega_D}+s(Q_h\boldsymbol{u},\boldsymbol{v})\\
&\quad+<\mu\mathbb{K}^{-1/2}(Q_b\boldsymbol{u}_S)\cdot\hat{\mathbf{t}},\boldsymbol{v}_b\cdot\hat{\mathbf{t}}>_{\Gamma_{SD}}-(\nabla_w\cdot\boldsymbol{v},\mathbb{Q}_h p)\\
&=2\nu(\Pi_h D(\boldsymbol{u}),\nabla_w(\boldsymbol{v}))_{\Omega_S}+(\mathbb{K}^{-1}Q_0\boldsymbol{u},\boldsymbol{v}_0)_{\Omega_D}+s(Q_h\boldsymbol{u},\boldsymbol{v})\\
&\quad+<\mu\mathbb{K}^{-1/2}(Q_b\boldsymbol{u}_S)\cdot\hat{\mathbf{t}},\boldsymbol{v}_b\cdot\hat{\mathbf{t}}>_{\Gamma_{SD}}-(\nabla_w\cdot\boldsymbol{v},\mathbb{Q}_h p).
\end{aligned}\tag{3.13}$$

Note that by condition (3.1) and the properties of L^2 projections,

$$\begin{aligned}
&2\nu(\Pi_h D(\boldsymbol{u}),\nabla_w(\boldsymbol{v}))_{\Omega_S}\\
&=2\nu\sum_{K\in\mathcal{T}_h^S}\Big(-(\boldsymbol{v}_0,\nabla\cdot(\Pi_h D(\boldsymbol{u})))_K+<\boldsymbol{v}_b,\Pi_h D(\boldsymbol{u})\mathbf{n}>_{\partial K}\Big)\\
&=2\nu\sum_{K\in\mathcal{T}_h^S}\Big((\nabla\boldsymbol{v}_0,\Pi_h D(\boldsymbol{u}))_K-<\boldsymbol{v}_0-\boldsymbol{v}_b,\Pi_h D(\boldsymbol{u})\mathbf{n}>_{\partial K}\Big)\\
&=2\nu\sum_{K\in\mathcal{T}_h^S}\Big((D(\boldsymbol{u}),D(\boldsymbol{v}_0))_K-<\boldsymbol{v}_0-\boldsymbol{v}_b,\Pi_h D(\boldsymbol{u})\mathbf{n}>_{\partial K}\Big),
\end{aligned}\tag{3.14}$$

and

$$\begin{aligned}
-(\nabla_w\cdot\boldsymbol{v},\mathbb{Q}_h p)&=\sum_{K\in\mathcal{T}_h}\Big((\boldsymbol{v}_0,\nabla(\mathbb{Q}_h p))_K-<\boldsymbol{v}_b\cdot\mathbf{n},\mathbb{Q}_h p>_{\partial K}\Big)\\
&=\sum_{K\in\mathcal{T}_h}\Big(-(\nabla\cdot\boldsymbol{v}_0,\mathbb{Q}_h p)_K+<(\boldsymbol{v}_0-\boldsymbol{v}_b)\cdot\mathbf{n},\mathbb{Q}_h p>_{\partial K}\Big)\\
&=\sum_{K\in\mathcal{T}_h}\Big(-(\nabla\cdot\boldsymbol{v}_0,p)_K+<(\boldsymbol{v}_0-\boldsymbol{v}_b)\cdot\mathbf{n},\mathbb{Q}_h p>_{\partial K}\Big).
\end{aligned}\tag{3.15}$$

Substituting (3.14) and (3.15) into (3.13), and then using (3.12), this completes the proof of the lemma. □

Finally, we have

Lemma 3.7. *The solution $\boldsymbol{u}$ to problem (2.1) satisfies*

$$b_h(Q_h\boldsymbol{u},q)=-(g,q),$$

for all $q\in\Psi_h$.

Proof By Lemma 3.4 and inequality (3.1), we have

$$b_h(Q_h\boldsymbol{u},q)=-(\nabla_w\cdot(Q_h\boldsymbol{u}),q)=-(\pi_h(\nabla\cdot\boldsymbol{u}),q)=-(\nabla\cdot\boldsymbol{u},q)=-(g,q).$$

This completes the proof of the lemma. □

4. Error analysis

In this section we derive an error estimation of the weak Galerkin approximation (3.5). Let $\boldsymbol{u}$, p be the solution to problem (2.1), and $\boldsymbol{u}_h = \{\boldsymbol{u}_0, \boldsymbol{u}_b\}$, p_h be the solution to the weak Galerkin formulation (3.5). Define the error by

$$e_{\boldsymbol{u}} = Q_h\boldsymbol{u} - \boldsymbol{u}_h = \{Q_0\boldsymbol{u} - \boldsymbol{u}_0, Q_b\boldsymbol{u} - \boldsymbol{u}_b\}, \qquad e_p = \mathbb{Q}p - p_h.$$

Then by Equation (3.5), Lemma 3.6 and 3.7, we clearly have

(4.1)
$$\begin{aligned} &a_h(e_{\boldsymbol{u}}, \boldsymbol{v}) + b_h(\boldsymbol{v}, e_p) \\ &\qquad = s(Q_h\boldsymbol{u}, \boldsymbol{v}) + l_S(\boldsymbol{v}) - l_D(\boldsymbol{v}) - l_{div}(\boldsymbol{v}) - l_I(\boldsymbol{v}) && \text{for all } \boldsymbol{v} \in \boldsymbol{V}_h, \\ &b_h(e_{\boldsymbol{u}}, q) = 0 && \text{for all } q \in \Psi_h. \end{aligned}$$

We shall first derive an upper bound for the right-hand side of (4.1). To this end, we start from getting an upper bound of $\left(\sum_{K\in\mathcal{T}_h^S} h_K^{-1}\|\boldsymbol{v}_0 - \boldsymbol{v}_b\|_{\partial K}^2\right)^{1/2}$, for any $\boldsymbol{v} \in \boldsymbol{V}_h$. From the definition of Q_b and $\|\cdot\|_{\boldsymbol{V}_h}$, it is clear that

Lemma 4.1. *If $\alpha_S = \beta$, then for all $\boldsymbol{v} \in \boldsymbol{V}_h$ we have*

$$\left(\sum_{K\in\mathcal{T}_h^S} h_K^{-1}\|\boldsymbol{v}_0 - \boldsymbol{v}_b\|_{\partial K}^2\right)^{1/2} \lesssim \|\boldsymbol{v}\|_{\boldsymbol{V}_h}.$$

We would like to derive the same bound for $\alpha_S = \beta + 1$, which turns out to be much more complicated and requires a discrete Korn's inequality. The proof of the following lemma is too long and hence is postponed to Appendix A.

Lemma 4.2. *When $\beta \geq 1$, $\alpha_S = \beta + 1$ and assume that all $K \in \mathcal{T}_h^S$ are affine homeomorphic to a fixed finite set of reference polygons, then for all $\boldsymbol{v} \in \boldsymbol{V}_h$ we have*

$$\left(\sum_{K\in\mathcal{T}_h^S} h_K^{-1}\|\boldsymbol{v}_0 - \boldsymbol{v}_b\|_{\partial K}^2\right)^{1/2} \lesssim \|\boldsymbol{v}\|_{\boldsymbol{V}_h}.$$

For the case $\beta = 0$ and $\alpha_S = 1$, the discrete Korn's inequality fails and we do not know if the same result as in lemmas (4.1) and (4.2) holds or not.

Using lemmas (4.1) and (4.2), we have

Lemma 4.3. *Let $\boldsymbol{u}$, p be the solution to problem (2.1) and $\boldsymbol{v} \in \boldsymbol{V}_h$, then we have*

$$\begin{aligned} s(Q_h\boldsymbol{u}, \boldsymbol{v}) &\lesssim \left(h^{r_S}\|\boldsymbol{u}\|_{r_S+1,\Omega_S} + h^{r_D}\|\boldsymbol{u}\|_{r_D+1,\Omega_D}\right)\|\boldsymbol{v}\|_{\boldsymbol{V}_h}, \\ l_S(\boldsymbol{v}) &\lesssim h^{r_\beta+1}\|\boldsymbol{u}\|_{r_\beta+2,\Omega_S}\|\boldsymbol{v}\|_{\boldsymbol{V}_h}, \\ l_D(\boldsymbol{v}) &\lesssim h^{r_D+1}\|\boldsymbol{u}\|_{r_D+1,\Omega_D}\|\boldsymbol{v}\|_{\boldsymbol{V}_h}, \\ l_{div}(\boldsymbol{v}) &\lesssim \left(h^{t_S+1}\|p\|_{t_S+1,\Omega_S} + h^{t_D+1}\|p\|_{t_D+1,\Omega_S}\right)\|\boldsymbol{v}\|_{\boldsymbol{V}_h}, \\ l_I(\boldsymbol{v}) &\lesssim h^{r_\beta+1}\|\boldsymbol{u}\|_{r_\beta+1,\Gamma_{SD}}\|\boldsymbol{v}\|_{\boldsymbol{V}_h}. \end{aligned}$$

where $0 \leq r_S \leq \alpha_S$, $0 \leq r_D \leq \alpha_D$, $0 \leq r_\beta \leq \beta$, $0 \leq t_S \leq \gamma_S$ and $0 \leq t_D \leq \gamma_D$.

Proof By the definition of $s(\cdot,\cdot)$, the property of Q_b, the Schwartz inequality, inequality (3.11), and the approximation property of Q_0, we have

$$\begin{aligned}
s(Q_h\boldsymbol{u},\boldsymbol{v}) &= \rho_S \sum_{K\in\mathcal{T}_h^S} h_K^{-1} < Q_0\boldsymbol{u}-\boldsymbol{u}, Q_b\boldsymbol{v}_0-\boldsymbol{v}_b >_{\partial K} \\
&\quad + \rho_D \sum_{K\in\mathcal{T}_h^D} h_K^{-1} < (Q_0\boldsymbol{u}-\boldsymbol{u})\cdot\mathbf{n}, (Q_b\boldsymbol{v}_0-\boldsymbol{v}_b)\cdot\mathbf{n} >_{\partial K} \\
&\lesssim \rho_S \left(\sum_{K\in\mathcal{T}_h^S} h_K^{-1}\|Q_0\boldsymbol{u}-\boldsymbol{u}\|_{\partial K}^2\right)^{1/2} \left(\sum_{K\in\mathcal{T}_h^S} h_K^{-1}\|Q_b\boldsymbol{v}_0-\boldsymbol{v}_b\|_{\partial K}^2\right)^{1/2} \\
&\quad + \rho_D \left(\sum_{K\in\mathcal{T}_h^D} h_K^{-1}\|Q_0\boldsymbol{u}-\boldsymbol{u}\|_{\partial K}^2\right)^{1/2} \left(\sum_{K\in\mathcal{T}_h^D} h_K^{-1}\|(Q_b\boldsymbol{v}_0-\boldsymbol{v}_b)\cdot\mathbf{n}\|_{\partial K}^2\right)^{1/2} \\
&\lesssim \left(h^{r_S}\|\boldsymbol{u}\|_{r_S+1,\Omega_S} + h^{r_D}\|\boldsymbol{u}\|_{r_D+1,\Omega_D}\right)\|\boldsymbol{v}\|_{\boldsymbol{V}_h},
\end{aligned}$$

where $0\le r_S\le\alpha_S$ and $0\le r_D\le\alpha_D$.

Next, by using the property of L^2 projection and lemmas 4.1-4.2, we have

$$\begin{aligned}
l_S(\boldsymbol{v}) &= 2\nu \sum_{K\in\mathcal{T}_h^S} < \boldsymbol{v}_0-\boldsymbol{v}_b, (D(\boldsymbol{u})-\Pi_h D(\boldsymbol{u}))\mathbf{n} >_{\partial K} \\
&\lesssim \left(\sum_{K\in\mathcal{T}_h^S} h_K^{-1}\|\boldsymbol{v}_0-\boldsymbol{v}_b\|_{\partial K}^2\right)^{1/2} \left(\sum_{K\in\mathcal{T}_h^S} h_K\|(D(\boldsymbol{u})-\Pi_h D(\boldsymbol{u}))\|_{\partial K}^2\right)^{1/2}, \\
&\lesssim h^{r_\beta+1}\|\boldsymbol{u}\|_{r_\beta+2,\Omega_S}\|\boldsymbol{v}\|_{\boldsymbol{V}_h},
\end{aligned}$$

where $0\le r_\beta\le\beta$. The estimate for $l_D(\boldsymbol{v})$ follows directly from the approximation property of Q_0. Similarly

$$\begin{aligned}
l_{div}(\boldsymbol{v}) &= \sum_{K\in\mathcal{T}_h} < (\boldsymbol{v}_0-\boldsymbol{v}_b)\cdot\mathbf{n}, p-\mathbb{Q}_h p >_{\partial K} \\
&\lesssim \left(\sum_{K\in\mathcal{T}_h^S} h_K^{-1}\|\boldsymbol{v}_0-\boldsymbol{v}_b\|_{\partial K}^2\right)^{1/2} h^{t_S+1}\|p\|_{t_S+1,\Omega_S} \\
&\quad + \left(\sum_{K\in\mathcal{T}_h^D} h_K^{-1}\|(\boldsymbol{v}_0-\boldsymbol{v}_b)\cdot\mathbf{n}\|_{\partial K}^2\right)^{1/2} h^{t_D+1}\|p\|_{t_D+1,\Omega_S} \\
&\lesssim \left(h^{t_S+1}\|p\|_{t_S+1,\Omega_S} + h^{t_D+1}\|p\|_{t_D+1,\Omega_S}\right)\|\boldsymbol{v}\|_{\boldsymbol{V}_h},
\end{aligned}$$

where $0\le t_S\le\gamma_S$ and $0\le t_D\le\gamma_D$.

Finally,

$$\begin{aligned}
l_I(\boldsymbol{v}) &=< \mu\mathbb{K}^{-1/2}(\boldsymbol{u}_S-Q_b\boldsymbol{u}_s)\cdot\hat{\mathbf{t}}, \boldsymbol{v}_b\cdot\hat{\mathbf{t}} >_{\Gamma_{SD}} \\
&\lesssim \|\boldsymbol{u}_s-Q_b\boldsymbol{u}_s\|_{\Gamma_{SD}}\|\boldsymbol{v}\|_{\boldsymbol{V}_h} \\
&\lesssim h^{r_\beta+1}\|\boldsymbol{u}\|_{r_\beta+1,\Gamma_{SD}}\|\boldsymbol{v}\|_{\boldsymbol{V}_h}.
\end{aligned}$$

This completes the proof of the lemma. □

Now we are able to write the error estimate:

Theorem 4.1. *Let α_s and β satisfy the conditions in Lemma 4.1 and 4.2, then the error $e_{\boldsymbol{u}}$ and e_p satisfies*

$$\begin{aligned}\|e_{\boldsymbol{u}}\|_{\boldsymbol{V}_h} + \|e_p\| \lesssim\ & h^{r_S}\|\boldsymbol{u}\|_{r_S+1,\Omega_S} + h^{r_D}\|\boldsymbol{u}\|_{r_D+1,\Omega_D} \\ & + h^{r_\beta+1}(\|\boldsymbol{u}\|_{r_\beta+2,\Omega_S} + \|\boldsymbol{u}\|_{r_\beta+1,\Gamma_{SD}}) \\ & + h^{t_S+1}\|p\|_{t_S+1,\Omega_S} + h^{t_D+1}\|p\|_{t_D+1,\Omega_S},\end{aligned}$$

where $0 \le r_S \le \alpha_S$, $0 \le r_D \le \alpha_D$, $0 \le r_\beta \le \beta$, $0 \le t_S \le \gamma_S$ and $0 \le t_D \le \gamma_D$.

Proof By setting $\boldsymbol{v} = e_{\boldsymbol{u}}$ and $q = e_p$ in (4.1) and then subtract these two equations, we have

$$\|e_{\boldsymbol{u}}\|^2_{\boldsymbol{V}_h} = a_h(e_{\boldsymbol{u}}, e_{\boldsymbol{u}}) = s(Q_h\boldsymbol{u}, e_{\boldsymbol{u}}) + l_S(e_{\boldsymbol{u}}) - l_D(e_{\boldsymbol{u}}) - l_{div}(e_{\boldsymbol{u}}) - l_I(e_{\boldsymbol{u}}).$$

Applying Lemma 4.3, this completes the proof for $\|e_{\boldsymbol{u}}\|_{\boldsymbol{V}_h}$.

To estimate $\|e_p\|$, note that from (4.1), we have

$$\begin{aligned}& b_h(\boldsymbol{v}, e_p) \\ =& s(Q_h\boldsymbol{u}, \boldsymbol{v}) + l_S(\boldsymbol{v}) - l_D(\boldsymbol{v}) - l_{div}(\boldsymbol{v}) - l_I(\boldsymbol{v}) - a_h(e_{\boldsymbol{u}}, \boldsymbol{v}) \\ \lesssim& \Big(h^{r_S}\|\boldsymbol{u}\|_{r_S+1,\Omega_S} + h^{r_D}\|\boldsymbol{u}\|_{r_D+1,\Omega_D} + h^{r_\beta+1}(\|\boldsymbol{u}\|_{r_\beta+2,\Omega_S} + \|\boldsymbol{u}\|_{r_\beta+1,\Gamma_{SD}}) \\ & + h^{t_S+1}\|p\|_{t_S+1,\Omega_S} + h^{t_D+1}\|p\|_{t_D+1,\Omega_S} + \|e_{\boldsymbol{u}}\|_{\boldsymbol{V}_h} \Big) \|\boldsymbol{v}\|_{\boldsymbol{V}_h}.\end{aligned}$$

Then by the discrete inf-sup condition stated in Lemma 3.5, this completes the proof for $\|e_p\|$. □

Remark 4.1. *Using the condition (3.1), one can see that, assuming the solution to (2.1) be as smooth as possible, we expect to have*

$$\|e_{\boldsymbol{u}}\|_{\boldsymbol{V}_h} + \|e_p\| \lesssim h^\beta + h^{\gamma_S+1} + h^{\gamma_D+1}.$$

Therefore, the best choice seems to be setting $\alpha_S = \alpha_D = \beta = j$ and $\gamma_S = \gamma_D = j-1$, for $j \ge 1$.

5. Numerical results

In this section we report some numerical results from solving the following test problem. Let $\Omega_S = (0,\pi)\times(0,1)$, $\Omega_D = (0,\pi)\times(-1,0)$ and the interface be $\Gamma_{SD} = \{0 < x < \pi,\, y = 0\}$. Set the coefficients to be

$$\nu = 1, \qquad \mathbb{K} = I, \qquad \mu = 1.$$

Under the given domain and coefficients, the following set of functions is known [9] to satisfy the coupled Darcy-Stokes equation (2.1) with the interface conditions (2.3)-(2.5):

$$\boldsymbol{u}_S = \begin{bmatrix} v'(y)\cos x \\ v(y)\sin x \end{bmatrix} \quad \text{where} \qquad v(y) = \frac{1}{\pi^2}\sin^2(\pi y) - 2,$$

$$p_S = \sin x\, \sin y,$$

$$p_D = (e^y - e^{-y})\sin x \qquad \text{and} \qquad \boldsymbol{u}_D = -\nabla p_D.$$

Use this set of functions, one can compute the force functions $\boldsymbol{f}$ and g, as well as the boundary conditions $\boldsymbol{u}_S|_{\Gamma_S}$ and $\boldsymbol{u}_D \cdot \mathbf{n}|_{\Gamma_D}$. This gives a complete set of data for the coupled Darcy-Stokes problem (2.1)-(2.5), with the exact solution known. Of course, we need to subtract p by $\int_\Omega p\,dx$ in order to make it mean value free.

We test the weak Galerkin approximation (3.5) for this test problem with the following settings. Both the Stokes and the Darcy side are divided into $n \times n$ grids, which combined together forms a $(2n) \times n$ rectangular mesh. The weak Galerkin space is chosen so that

$$\alpha_S = \alpha_D = \beta = 1, \qquad \gamma_S = \gamma_D = 0.$$

According to the analysis given in this paper, the discrete system (3.5) is well-posed and we expect it to provide an approximation error of at least

$$\|e_{\boldsymbol{u}}\|_{\boldsymbol{V}_h} + \|e_p\| = O(h).$$

The error terms in the theoretical analysis are defined as $e_{\boldsymbol{u}} = Q_h\boldsymbol{u} - \boldsymbol{u}_h$ and $e_p = \mathbb{Q}p - p_h$. In practice, for simplicity, we made some modification. Define by $I_h\boldsymbol{u}$ an interpolation of $\boldsymbol{u}$ in $\boldsymbol{V}_h$ such that: its value on an edge is the usual P_1 nodal value interpolation using two end points of the edge; and its value on a rectangle is the P_1 nodal value interpolation using three vertices of the rectangle, the lower-left corner, the lower-right corner, and the upper-left corner. Define by J_hp an interpolation of p in Ψ_h such that its value in each rectangle is a constant equal to the value of p at the center of this rectangle. Then, we consider the following modified error terms

$$\hat{e}_{\boldsymbol{u}} = I_h\boldsymbol{u} - \boldsymbol{u}_h, \qquad \hat{e}_p = J_hp - p_h.$$

By the approximation property of projections and interpolations, we expect that $\|\hat{e}_{\boldsymbol{u}}\|_{\boldsymbol{V}_h} + \|\hat{e}_p\|$ has the same order as $\|e_{\boldsymbol{u}}\|_{\boldsymbol{V}_h} + \|e_p\|$.

We computed the following norms and seminorms of the error: on the Stokes side are $\|\nabla_w\hat{e}_{\boldsymbol{u}}\|_{\Omega_S}$, $\|(\hat{e}_{\boldsymbol{u}})_0\|_{\Omega_S}$, and $\|\hat{e}_p\|_{\Omega_S}$; on the Darcy side are $\|(\hat{e}_{\boldsymbol{u}})_0\|_{\Omega_D}$ and $\|\hat{e}_p\|_{\Omega_D}$. According to the theoretical error estimate, we expect at least

$$\|\nabla_w\hat{e}_{\boldsymbol{u}}\|_{\Omega_S} = O(h), \qquad \|\hat{e}_p\|_{\Omega_S} = O(h),$$
$$\|(\hat{e}_{\boldsymbol{u}})_0\|_{\Omega_D} = O(h), \qquad \|\hat{e}_p\|_{\Omega_D} = O(h).$$

We did not have theoretical error estimate for $\|(\hat{e}_{\boldsymbol{u}})_0\|_{\Omega_S}$, although by experience from using the duality argument, we expect that the optimal case for this term is

$$\|(\hat{e}_{\boldsymbol{u}})_0\|_{\Omega_S} = O(h^2).$$

In the numerical experiment, we picked the stabilization constants $\rho_S = \rho_D = \rho$ to be 0.01, 1 and 100. Numerical results are reported in the tables 1-3 and Figure 2.

In Figure 2, we conveniently denote the norms $\|\nabla_w\hat{e}_{\boldsymbol{u}}\|_{\Omega_S}$, $\|(\hat{e}_{\boldsymbol{u}})_0\|_{\Omega_S}$, $\|\hat{e}_p\|_{\Omega_S}$, $\|(\hat{e}_{\boldsymbol{u}})_0\|_{\Omega_D}$, $\|\hat{e}_p\|_{\Omega_D}$ by H1 $\boldsymbol{u}_S$, L2 $\boldsymbol{u}_S$, L2 p_S, L2 $\boldsymbol{u}_D$, and L2 p_D. For $\rho = 1$ and $\rho = 100$, the asymptotic behavior of the errors are clearly seen from Figure 2, as the curves are almost straight lines. For $\rho = 0.01$, it seems that the asymptotic behavior deteriorates when h is large. But as h becomes smaller, the convergence rates get better. However, we notice that for all three values of ρ, the orders of $\|(\hat{e}_{\boldsymbol{u}})_0\|_{\Omega_S}$ are approximately equal to or higher than $O(h^2)$, while the order of other errors are approximately equal to or higher than $O(h)$, which are guaranteed by the theoretical analysis. One important and interesting question is how to pick

TABLE 1. Error for $\rho = 0.01$. Order $O(h^r)$ computed from $n = 16$ to $n = 128$.

n	$\|\nabla_w \hat{e}_{\boldsymbol{u}}\|_{\Omega_S}$	$\|(\hat{e}_{\boldsymbol{u}})_0\|_{\Omega_S}$	$\|\hat{e}_p\|_{\Omega_S}$	$\|(\hat{e}_{\boldsymbol{u}})_0\|_{\Omega_D}$	$\|\hat{e}_p\|_{\Omega_D}$
8	0.76224	2.26639	0.84301	2.54274	0.91539
16	0.30306	0.26226	0.25407	1.56049	0.56486
32	0.14960	0.03332	0.08316	0.65226	0.24125
64	0.07461	0.00486	0.02365	0.20346	0.07536
128	0.03719	0.00089	0.00615	0.05691	0.02016
$O(h^r)$, $r =$	1.0083	2.7383	1.7917	1.6012	1.6103

TABLE 2. Error for $\rho = 1$. Order $O(h^r)$ computed from $n = 8$ to $n = 128$.

n	$\|\nabla_w \hat{e}_{\boldsymbol{u}}\|_{\Omega_S}$	$\|(\hat{e}_{\boldsymbol{u}})_0\|_{\Omega_S}$	$\|\hat{e}_p\|_{\Omega_S}$	$\|(\hat{e}_{\boldsymbol{u}})_0\|_{\Omega_D}$	$\|\hat{e}_p\|_{\Omega_D}$
8	0.56159	0.03842	0.07539	0.18953	0.07511
16	0.28729	0.00850	0.02055	0.06858	0.01953
32	0.14443	0.00204	0.00538	0.02925	0.00492
64	0.07231	0.00050	0.00137	0.01381	0.00123
128	0.03616	0.00012	0.00035	0.00678	0.00031
$O(h^r)$, $r =$	0.9904	2.0622	1.9402	1.1924	1.9846

TABLE 3. Error for $\rho = 100$. Order $O(h^r)$ computed from $n = 8$ to $n = 128$.

n	$\|\nabla_w \hat{e}_{\boldsymbol{u}}\|_{\Omega_S}$	$\|(\hat{e}_{\boldsymbol{u}})_0\|_{\Omega_S}$	$\|\hat{e}_p\|_{\Omega_S}$	$\|(\hat{e}_{\boldsymbol{u}})_0\|_{\Omega_D}$	$\|\hat{e}_p\|_{\Omega_D}$
8	0.47789	0.03379	0.31537	0.06226	0.16416
16	0.24268	0.01117	0.09409	0.02190	0.04211
32	0.12079	0.00325	0.02371	0.00950	0.01061
64	0.06017	0.00086	0.00583	0.00457	0.00264
128	0.03004	0.00022	0.00144	0.00227	0.00066
$O(h^r)$, $r =$	0.9995	1.8266	1.9552	1.1817	1.9921

the best parameter ρ. One may use the techniques proposed in [27]. It is beyond the scope of this paper, but suitable for a future research topic.

From the results of $\rho = 1$ and $\rho = 100$, it seems that the both $\|\hat{e}_p\|_{\Omega_S}$ and $\|\hat{e}_p\|_{\Omega_D}$ also achieves $O(h^2)$ convergence. This might be caused by super-convergence on uniform rectangular meshes. We will not explore the super-convergence effect here. The super-convergence of a primal based formulation for the Darcy-Stokes equation has been discussed in [9].

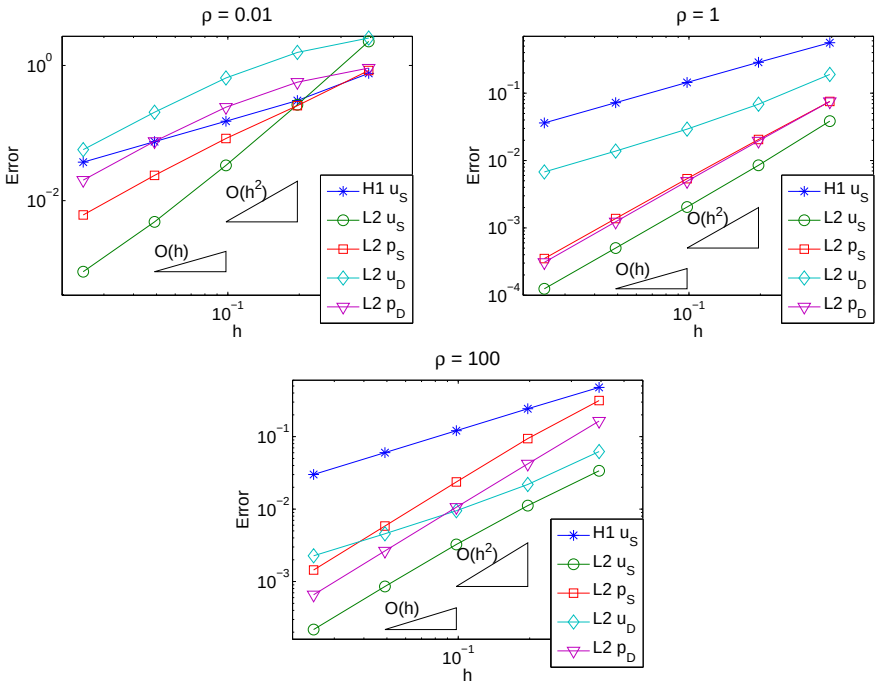

FIGURE 2. Convergence rates, $\rho = 0.01$, 1 and 100.

APPENDIX A. PROOF OF LEMMA 4.2

By using the triangle inequality, Equation (3.11), the inverse inequality, the property of Q_b and Q_0, for all $\boldsymbol{v} \in \boldsymbol{V}_h$ we have

$$\begin{aligned}
\sum_{K\in\mathcal{T}_h^S} h_K^{-1}\|\boldsymbol{v}_0-\boldsymbol{v}_b\|_{\partial K}^2 &\lesssim \sum_{K\in\mathcal{T}_h^S} h_K^{-1}(\|\boldsymbol{v}_0-Q_b\boldsymbol{v}_0\|_{\partial K}^2+\|Q_b\boldsymbol{v}_0-\boldsymbol{v}_b\|_{\partial K}^2)\\
&\lesssim \sum_{K\in\mathcal{T}_h^S} h_K^{-1}\|\boldsymbol{v}_0-Q_0\boldsymbol{v}_0\|_{\partial K}^2+\|\boldsymbol{v}\|_{\boldsymbol{V}_h}^2\\
&\lesssim \sum_{K\in\mathcal{T}_h^S} h_K^{-2}\|\boldsymbol{v}_0-Q_0\boldsymbol{v}_0\|_K^2+\|\boldsymbol{v}\|_{\boldsymbol{V}_h}^2\\
&\lesssim \sum_{K\in\mathcal{T}_h^S} \|\nabla\boldsymbol{v}_0\|_K^2+\|\boldsymbol{v}\|_{\boldsymbol{V}_h}^2.
\end{aligned}$$

Now the difficulty is to bound $\sum_{K\in\mathcal{T}_h^S}\|\nabla\boldsymbol{v}_0\|_K^2$ by $\|\boldsymbol{v}\|_{\boldsymbol{V}_h}^2$. By Lemma A.2 in [41], one has $\|\nabla\boldsymbol{v}_0\|_K^2 \lesssim \|\nabla_w\boldsymbol{v}\|_K^2 + h_K^{-1}\|Q_b\boldsymbol{v}_0-\boldsymbol{v}_b\|_{\partial K}^2$ and this seems to be a possible solution. However, on second thought, $\|\nabla_w\boldsymbol{v}\|_{\Omega_S}$ is not necessarily bounded by $\|\boldsymbol{v}\|_{\boldsymbol{V}_h}$, which indeed contains $\|D_w(\boldsymbol{v})\|_{\Omega_S}$. Here one obviously needs a discrete Korn's inequality involving the weak gradient.

It turns out to be easier to first apply a discrete Korn's inequality to $\nabla\boldsymbol{v}_0$ instead of trying to bound it using $\nabla_w\boldsymbol{v}$. By [4], when all $K\in\mathcal{T}_h^S$ are affine homeomorphic

to a fixed finite set of reference polygons, one has

$$\begin{aligned}\sum_{K\in\mathcal{T}_h^S}\|\nabla \boldsymbol{v}_0\|_K^2 \lesssim \sum_{K\in\mathcal{T}_h^S}\|D(\boldsymbol{v}_0)\|_K^2 + \sup_{\substack{\mathbf{m}\in RM,\ \|\mathbf{m}\|_{\Gamma_S}=1\\ \int_{\Gamma_S}\mathbf{m}\,ds=\mathbf{0}}}\left(\int_{\Gamma_S}\boldsymbol{v}_0\cdot\mathbf{m}\,ds\right)^2\\ +\sum_{e\in\mathcal{E}_{0,h}^S}\|\pi_e[\boldsymbol{v}_0]\|_e^2,\end{aligned}\tag{A.1}$$

where RM is the space of rigid body motions, π_e is the L^2 projection onto $(P_1(e))^2$ and $[\cdot]$ denotes the jump on edges. Next, we estimate the right-hand side of (A.1) one-by-one.

Similar to Lemma A.2 in [41], we have

Lemma A.1. *For $\boldsymbol{v}\in\boldsymbol{V}_h$ and any $K\in\mathcal{T}_h^S$, we have*

$$\|D(\boldsymbol{v}_0)\|_K \lesssim \|D_w(\boldsymbol{v})\|_K + h_K^{-1/2}\|Q_b\boldsymbol{v}_0-\boldsymbol{v}_b\|_{\partial K}.$$

Proof. Note that

$$\begin{aligned}(D(\boldsymbol{v}_0),\,D(\boldsymbol{v}_0))_K &= (D(\boldsymbol{v}_0),\,\nabla\boldsymbol{v}_0)_K\\ &= -(\boldsymbol{v}_0,\,\nabla\cdot D(\boldsymbol{v}_0))_K + <\boldsymbol{v}_0,\,D(\boldsymbol{v}_0)\cdot\mathbf{n}>_{\partial K}\\ &= (\nabla_w\boldsymbol{v},\,D(\boldsymbol{v}_0))_K + <\boldsymbol{v}_0-\boldsymbol{v}_b,\,D(\boldsymbol{v}_0)\cdot\mathbf{n}>_{\partial K}\\ &= (D_w(\boldsymbol{v}),\,D(\boldsymbol{v}_0))_K + <Q_b\boldsymbol{v}_0-\boldsymbol{v}_b,\,D(\boldsymbol{v}_0)\cdot\mathbf{n}>_{\partial K}.\end{aligned}$$

The lemma then follows from the Schwarz inequality, Inequality (3.11) and the inverse inequality. □

The estimate of the second and the third term in the right-hand side of (A.1) requires $\beta\geq 1$. Indeed, when $\beta\geq 1$, since $RM\subset(P_\beta)^2$ and $\boldsymbol{v}_b$ vanishes on Γ_S, we have

$$\begin{aligned}\sup_{\substack{\mathbf{m}\in RM,\ \|\mathbf{m}\|_{\Gamma_S}=1\\ \int_{\Gamma_S}\mathbf{m}\,ds=\mathbf{0}}}\left(\int_{\Gamma_S}\boldsymbol{v}_0\cdot\mathbf{m}\,ds\right)^2 &= \sup_{\substack{\mathbf{m}\in RM,\ \|\mathbf{m}\|_{\Gamma_S}=1\\ \int_{\Gamma_S}\mathbf{m}\,ds=\mathbf{0}}}\left(\int_{\Gamma_S}(Q_b\boldsymbol{v}_0-\boldsymbol{v}_b)\cdot\mathbf{m}\,ds\right)^2\\ &\lesssim \|Q_b\boldsymbol{v}_0-\boldsymbol{v}_b\|_{\Gamma_S}^2,\end{aligned}\tag{A.2}$$

and since $\pi_e[\boldsymbol{v}_0]\in(P_1(e))^2\subset(P_\beta(e))^2$, we have

$$\begin{aligned}\sum_{e\in\mathcal{E}_{0,h}^S}\|\pi_e[\boldsymbol{v}_0]\|_e^2 &\lesssim \sum_{e\in\mathcal{E}_{0,h}^S}\|Q_b[\boldsymbol{v}_0]\|_e^2\\ &\lesssim \sum_{K\in\mathcal{T}_h^S}\|Q_b\boldsymbol{v}_0-\boldsymbol{v}_b\|_{\partial K}^2.\end{aligned}\tag{A.3}$$

Combining the above analysis, by using inequalities (A.1), (A.2), (A.3), Lemma A.1 and the fact that $O(1)\leq h_K^{-1/2}$, this completes the proof of Lemma 4.2.

ACKNOWLEDGMENTS: Chen is supported by the Key Project National Science Foundation of China(91130004) and Natural Science Foundation of China (11171077, 11331004). Wang thanks the Key Laboratory of Mathematics for Nonlinear Sciences (EZH1411108/001) of Fudan University, and the Ministry of Education of China & State Administration of Foreign Experts Affairs of China under the 111 project grant (B08018), for the support during her visit.

References

[1] T. Arbogast and D.S. Brunson, *A computational method for approximating a Darcy-Stokes system governing a vuggy porous medium*, Computational Geosciences, 11 (2007), 207–218.

[2] G.S. Beavers and D.D. Joseph, *Boundary conditions at a naturally permeable wall*, J. Fluid Mech., 30 (1967), 197–207.

[3] C. Bernardi, T.C. Rebollo, F. Hecht and Z. Mghazli, *Mortar finite element discretization of a model coupling Darcy and Stokes equations*, M2AN Math. Model. Numer. Anal., 42 (2008), 375–410.

[4] S. Brenner, *Korn's inequalities for piecewise H^1 vector fields*, Math. Comp., 247 (2003), 1067–1087.

[5] F. Brezzi and M. Fortin, *Mixed and Hybrid Finite Element Methods*, Springer-Verlag, New York-Berlin-Heidelberg, 1991.

[6] Y. Cao, M Gunzburger and X. He, *Robin-Robin domain decomposition methods for the steady-state Stokes-Darcy system with the Beavers-Joseph interface condition*, Numer. Math., 117 (2011), 601–629.

[7] Y. Cao, M Gunzburger and X. He, *Finite element approximations for Stokes-Darcy flow with Beavers-Joseph interface condition*, SIAM J. Numer. Anal., 47 (2010), 4239–4256.

[8] Y. Cao, M Gunzburger, F. Hua and X. Wang, *coupled Stokes-Darcy model with Beavers-Joseph interface boundary condition*, Comm. Math. Sci., 8 (2010), 1–25.

[9] W. Chen, P. Chen, M. Gunzburger and N. Yan, *Superconvergence analysis of FEMs for the Stokes-Darcy system*, Math. Methods Appl. Sci. 33 (2010), 1605–1617.

[10] W. Chen and X. Wang, *A parallel Robin-Robin domain decomposition method for the Stokes-Darcy system*, SIAM J. Numer. Anal., 49 (2011), 1064–1084.

[11] W. Chen and Y. Wang, *A posteriori error estimate for the H(div) conforming mixed finite element for the coupled Darcy-Stokes system*, J. Comp. Appl. Math., 255 (2014), 502–516.

[12] M. Discacciati and A. Quarteroni, *Navier-Stokes/Darcy Coupling: Modeling, Analysis, and Numerical Approximation*, Rev. Mat. Complut., 22 (2009), 315–426.

[13] M. Discacciati, A. Quarteroni And A. Valli, *Robin-Robin domain decomposition methods for the Stokes-Darcy coupling*, SIAM J. Numer. Anal., 45 (2007), 1246–1268.

[14] R. S. Falk, *Nonconforming Finite Element Methods for the Equations of Linear Elasticity*, Math. Comp. 57 (1991), 529–550.

[15] J. Galvis and M. Sarkis, *Non-matching mortar discretization analysis for the coupling Stokes-Darcy equations*, Electron. Trans. Numer. Anal., 26 (2007), 350–384.

[16] G.N. Gatica, S. Meddahi and R. Oyarzúa, *A conforming mixed finite-element method for the coupling of fluid flow with porous media flow*, IMA J. Numer. Anal., 29 (2009), 86–108.

[17] G.N. Gatica, R. Oyarzúa and F.-J. Sayas, *Convergence of a family of Galerkin discretizations for the Stokes-Darcy coupled problem*, Numer. Meth. Part. Diff. Eq., 27 (2011), 721–748.

[18] V. Girault, G. Kanschat and B. Riviére, *Error analysis for a monolithic discretization of coupled Darcy and Stokes problems*, IMA preprint 2390.

[19] V. Girault and P. Raviart, *Finite element methods for Navier-Stokes equations*, Springer-Verlag, Berlin-Heidelberg-New York-Tokyo, 1986.

[20] V. Girault and B. Riviére, *DG approximation of coupled Navier-Stokes and Darcy equations by Beaver-Joseph-Saffman interface condition*, SIAM J. Numer. Anal., 47 (2009), 2052–2089.

[21] W. Jäger and A. Mikelić, *On the boundary conditions at the contact interface between a porous medium and a free fluid*, Ann. Scuola Norm. Sup. Pisa Cl. Sci., 23 (1996), 403–465.

[22] W. Jäger and A. Mikelić, *On the interface boundary condition of Beavers, Joseph and Saffman*, SIAM J. Appl. Math., 60 (2000), 1111–1127.

[23] W. Jäger, A. Mikelić and N. Neuss, *Asymptotic analysis of the laminar viscous flow over a porous bed*, SIAM J. Sci. Comput., 22 (2001), 2006–2028.

[24] G. Kanschat and B. Rivière, *A strongly conservative finite element method for the coupling of Stokes and Darcy flow*, J. Comput. Phys., 229 (2010), 5933–5943.

[25] T. Karper, K.-A. Mardal and R. Winther, *Unified Finite Element Discretizations of Coupled Darcy-Stokes Flow*, Numer. Meth. Part. Diff. Eq., 25 (2008), 311–326.

[26] W.J. Layton, F. Schieweck and I. Yotov, *Coupling fluid flow with porous media flow*, SIAM J. Numer. Anal., 40 (2003), 2195–2218.

[27] R. Lazarov, S. Lu and S. Pereverzev, *On the balancing principle for some problems of numerical analysis*, Numer. Math., 106 (2007), 659–689.

[28] J. L. Lions and E. Magenes, *Non-homogeneous Boundary Value Problems and Applications*, Vol. 1, Springer-Verlag, New York-Heidelberg, 1972.
[29] A. Márquez, S. Meddahi and F.J. Sayas, *Strong coupling of finite element methods for the Stokes-Darcy problem*, IMA J. Numer. Anal., doi:10.1093/imanum/dru023
[30] *L. Mu, J. Wang, Y. Wang and X. Ye*, *A Weak Galerkin Mixed Finite Element Method for Biharmonic Equations*, Conference Proceeding for Numerical Solution of Partial Differential Equations: Theory, Algorithms and their Applications, Vol. 45 (2013), 247–277.
[31] L. Mu, J. Wang, and X. Ye, *Weak Galerkin finite element methods on polytopal meshes*, arXiv:1204.3655v2.
[32] L. Mu, X. Wang and Y. Wang, *Shape regularity conditions for polygonal/polyhedral meshes, exemplified in a discontinuous Galerkin discretization*, to appear in Numer. Methods. Part. Diff. Eq.
[33] L. Mu, J. Wang, Y. Wang and X. Ye, *A computational study of the weak Galerkin method for second order elliptic equations*, Numer. Algor., 63 (2013), 753–777.
[34] L.E. Payne and B. Straughan, *Analysis of the boundary condition at the interface between a viscous fluid and a porous medium and related modelling questions*, J. Math. Pures Appl., 77 (1998), 317–354.
[35] M. Mu and J. Xu, *A two-grid method of a mixed Stokes-Darcy model for coupling fluid flow with porous media flow*, SIAM J. Numer. Anal. 45 (2007), 1801–1813.
[36] B. Riviére, *Analysis of a discontinuous finite element method for the coupled Stokes and Darcy problems*, J. Sci. Comp., 22-23 (2005), 479–500.
[37] B. Riviére and I. Yotov, *Locally conservative coupling of Stokes and Darcy flows*, SIAM J. Numer. Anal., 42 (2005), 1959–1977.
[38] P.G. Saffman, *On the boundary condition at the interface of a porous medium*, Stud. Appl. Math., 1 (1971), 93–101.
[39] J. Wang and X. Ye, *A weak Galerkin finite element method for second-order elliptic problems*, J. Comput. Applied Math., 241 (2013), 103–115.
[40] J. Wang and X. Ye, *A Weak Galerkin mixed finite element method for second-order elliptic problems*, arXiv:1202.3655v1, to appear in Math Comp.
[41] J. Wang and X. Ye, *A Weak Galerkin Finite Element Method for the Stokes Equations*, arXiv:1302.2707v1.

Department of Mathematics, Fudan University, Shanghai, China
E-mail address: wbchen@fudan.edu.cn

Department of Mathematics, Fudan University, Shanghai, China
E-mail address: 07300180148@fudan.edu.cn

Department of Mathematics, Oklahoma State University, Stillwater, OK, USA
E-mail address: yqwang@math.okstate.edu